Utrecht University

Investigating the spread of stress on the work floor with the failure-recovery model: bistability, critical transitions and robustness.

Author:
Lisanne Hogeveen

Supervisors:
prof. dr. ir. Jason Frank*
dr. Heleen Wortelboer†
dr. Tanja Krone†

* Mathematical Institute, Utrecht University
† TNO

Master thesis
in
Mathematical Sciences

Written in combination with an internship at

TNO

January 24, 2018

Contents

Introduction

Many social, biological, and communication systems can be properly described by complex networks. In such a network, nodes represent individuals or organizations, and the links between the nodes mimic the interactions between them[25]. Typical processes that can be represented as networks are epidemic processes, searches, diffusion processes, synchronization, and spread of information, damage or disease[19].

In this thesis we will study the spread of stress on the work floor. We will look at different networks to find which network is most robust and interpret the answers to this question in the context of the spread of stress in the workplace.

We use a network to describe the relations between the individuals in an organization. In this thesis the nodes represent different individuals, and if two nodes are connected by a link this means that the two individuals depend on each other in some way. For example, the individuals may work in the same department or they may contribute to the same project. Two connected individuals are called neighbors, and the neighborhood of an individual consist of all its neighbors. An overload of stress of an individual can lead to improductivity or even a burnout, and the failure of one individual can start a cascade of failures throughout the network. We are interested in the influence of the network structure on the robustness of the network, defining robustness as the ability to function even when a large fraction of the network has failed. Therefore, we will study different network types which we distinguish by their local properties.

We will describe the dynamics of an organization by the failure-recovery model as in [19]. In this model, individuals can fail due to internal or external factors. Internal failure of an individual can be caused by personal issues, related to their own functioning. Individuals do not only suffer from stress induced by internal factors, but can also be influenced by external factors such as lack of support from their neighborhood. External failure means that an individual ceases to function because of outside influences. In this thesis, we regard the activity of the neighborhood of a node as an external factor. To be more specific, an individual has the possibility to collapse due to external failure if the number of active neighbors is smaller than some threshold.

External failure introduces local dependencies; that is, the effect that a single failed neighbor will have on a given individual depends critically on the neighborhood of the individual[35]. This feature is also found in percolation models, where damage spreads through the network. Nevertheless, the model is different from percolation models, as it includes internal failure: the possibility for a node to fail at random and independently of its neighbors.

Individuals also have the possibility to recover from failure. Proper restoration can prevent failure propagation through the entire network[18]. Also, it can lead to interesting dynamics such as bistability as pointed out in [26].

We will analytically describe the dynamics in the model in the framework of Continuous Time Markov Chains. We use the effective degree approach [15] to obtain a set of differential equations describing the change in active, internally failed and externally failed nodes. In addition to that, we use the Gillespie algorithm to perform stochastic simulations.

This research will contribute to the existing literature by investigating the robustness of different networks. We will study four types of networks, which we distinguish by their local properties. We consider networks with short characteristic path length and low clustering: Erdös-Rényi and regular networks. We also consider networks with short characteristic path length and high clustering: Watts-Strogatz networks. These three network types have a narrow degree distribution, therefore, we also consider Barabási networks with a broad degree distribution.

In the study of failure models where recovery is not possible, the robustness of different network types is studied in [9, 29, 36]. But for the failure-recovery model, the research in [21, 32] is limited to Erdös-Rényi and regular networks. In this thesis we aim to find which network is most robust and

interpret the answers to this question in the context of the spread of stress in the workplace.

The rest of this thesis is structured as follows. In chapter 1 we will introduce the failure-recovery model. In chapter 2 we will study the dynamics of the failure-recovery model on a regular network in which all nodes have the same degree. To decrease the size of the state space, we will use the effective degree approach. We will construct a set of differential equations, which we will solve numerically. We will also use a mean field approximation to illustrate the behavior of the system. In chapter 3 we will study the failure-recovery model for interconnected networks. The nodes in the interconnected networks depend on each other, therefore, we also consider dependency failure. We will use the effective degree approach to analytically study the model. Note that interconnected networks are only considered in this chapter. In chapter 4 we will introduce the Gillespie algorithm, which is needed for the stochastic simulations we will use to study networks with heterogeneous nodes. In chapter 5 we will consider different types of networks. We characterize a network by its local properties using the measures characteristic path length and clustering. Finally, chapter 6 is devoted to summarizing the results and interpreting the results in the context of the spread of stress in the workplace. Also, we will address some suggestions for further research.

Chapter 1

Model introduction

In this chapter we introduce the failure-recovery model, we fit the model into the framework of Continuous Time Markov Chains (CTMC). First, we will start with a formal introduction to CTMC. Next, we will introduce the failure-recovery model.

1.1 Continuous Time Markov Chains

In this section we define the CTMC $(X_t)_{t\geq 0}$ as in [23]. Let I be a countable set. Each $i \in I$ is called a state and I is called a state space. Let Q be the matrix that consist of the transition rates between the states, and choose the diagonal elements such that the rows sum to zero. More formally, $Q = (q_{ij} : i, j \in I)$ satisfies the following conditions

(i) $0 \leq q_{ii} < \infty$ for all i;

(ii) $q_{ij} \geq 0$ for all $i \neq j$;

(iii) $\sum_{j\in I} q_{ij} = 0$ for all i.

For all $n = 0, 1, \ldots$, all times $t_0, t_1, \ldots, t_{n+1}$ and all states defined at these times $i_0, i_1, \ldots, i_{n+1}$ holds

$$\mathbb{P}(X_{t_{n+1}} = i_{n+1} | X_{t_0} = i_0, X_{t_1} = i_1, \ldots, X_{t_n} = i_n) = \mathbb{P}(X_{t_{n+1}} = i_{n+1} | X_{t_n} = i_n). \tag{1.1}$$

So given the state of the process at any set of times prior to time t, the distribution of the process at time t only depends on the process at the most recent time prior to time t. Next, given that the chain starts at state i, it ends up at state j at time t with probability $p_{ij}(t)$. To be more specific,

$$\mathbb{P}(X_{t_{n+1}} = i_{n+1} | X_{t_n} = i_n) = p_{ij}(t_{n+1} - t_n). \tag{1.2}$$

This p_{ij} is related to Q by the forward equation

$$\frac{dP}{dt} = QP(t), \qquad P(0) = P_0, \tag{1.3}$$

where P_0 is the initial probability distribution defined on the state space.

1.2 Model introduction

In what follows, we assume networks of size $i = 1, \ldots, N$. The degree of node i is denoted by k_i, and the average degree of the nodes in the network is denoted by $\bar{k}$. Three fundamental assumptions of the failure-recovery model are as follows.

(i) A node fails independently of other nodes at rate p, this type of failure is referred to as *internal failure*.

(ii) A node fails at rate r if its neighborhood is damaged. The neighborhood of a node is damaged when its number of active neighbors is less than or equal to the absolute threshold m. For an illustration see figure 1.1. This type of failure is referred to as *external failure*.

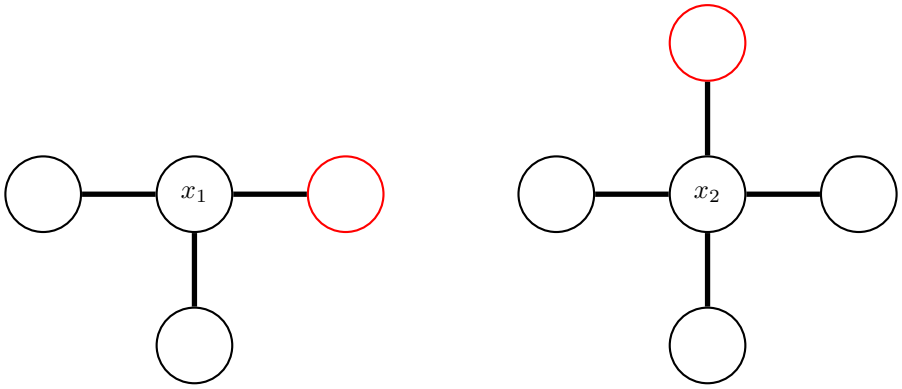

Figure 1.1: Illustration of the activity of the neighborhood for two nodes, for $m = 2$. Failed neighbors are marked red and active neighbors are marked black. Node x_1 has a damaged neighborhood, it fails externally at rate r. Node x_2 has a healthy neighborhood, it is not vulnerable to external failure.

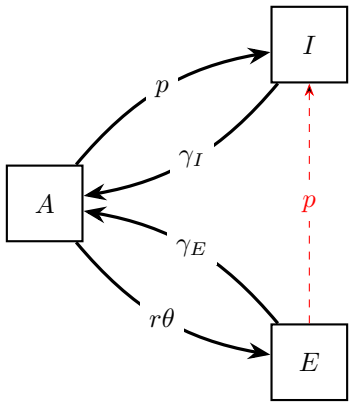

Figure 1.2: Possible state transitions of a node between the active (A), internally failed (I) and externally failed (E) state in the CTMC. The dashed red arrow indicates the transition from externally failed to internally failed, the inclusion of this transition is discussed in section 2.5.

(iii) Nodes can recover from failure. For internal failure the recovery rate equals γ_I and nodes recover from external failure at rate γ_E.

We denote the fraction of active, internally failed and externally failed nodes by A, I and E respectively. An illustration of all possible transitions between states and the corresponding rates is given in figure 1.2. Note that the transition displayed with a dashed red arrow is only included in section 2.5. $\Theta(x)$ is the Heaviside distribution which takes value 1 for non-negative values of x and value 0 for negative values of x, thus $\theta := \Theta(m - a)$ equals one when a node has a damaged neighborhood.

Note that in (ii) we use an absolute threshold m. In scale-free networks the degree distribution is very broad, a fractional threshold may be more appropriate than an absolute threshold[27]. In chapters 2 and 4 we will only consider regular networks (i.e. networks in which all nodes have the same degree), in which case the two thresholds come down to the same. In our context, nodes of high degree are considered to be less vulnerable against random failure. Therefore, we also assume an absolute threshold for networks with a broad degree distribution.

The failure-recovery model is also used in [32] in relation to epidemiology, with two modifications. First, [32] stipulates transition rates instead of transition probabilities, and second, individuals do not have the possibility to switch from externally failed to internally failed. In our context internal failure and external failure are assumed to be of different nature, therefore in section 2.5 we will also briefly address the possibility of internal failure for externally failed nodes.

In this thesis, we assume that nodes recover from failure at fixed rate. In [19] it is assumed that recovery happens after a fixed time, although adjustments of this assumption are made by others. For example, [3, 32] assume that recovery happens with a certain probability, [26] includes the fact that internal failure always carries the potential risk of being permanent, and [12] adopts targeted recovery in which nodes with high degree are iteratively recovered. Furthermore, in the case of a dynamic network, [31] stipulates the possibility of link formation (i.e. making new connections between nodes). Note that,

in real-world networks, not all nodes can be restored, owing for example to restoration difficulty and limited technological maturity[12, 14].

Further, instead of using the rate for internal failure p we will use the more convenient parameter p^* which is a function of p and γ_I. It is defined as $p^* = 1 - \exp(-p/\gamma_I)$, for a derivation see appendix A.1. Note that by this definition we can scale the state space such that $\gamma_I = 1$. This can be intuitively understood as follows: increasing the rate of internal failure has a similar effect as increasing the recovery rate γ_I; both lead to a smaller fraction of active nodes. Also, as found in [19], we assume that recovery from external failure is faster than recovery from internal failure, i.e. $\gamma_E > \gamma_I$. Similar to [19] we assume $\gamma_E = 0.01$.

To summarize: in this chapter we introduced the failure-recovery model in which nodes can fail due to internal and external failure, also nodes have the possibility to recover. In the following we will further investigate the dynamics within this model.

Chapter 2

Analytical results

To explore the qualitative behavior of the system, in this chapter we will analytically study the failure-recovery model as introduced in chapter 1. We will use the effective degree approach to reduce the size of the state space. First, we will derive a system of ODEs from which we will subsequently derive mean-field equations. Eventually we will find that the phase diagram can be divided into three regions where the system exhibits stable, bistable or oscillatory behavior.

2.1 Effective degree approach

As discussed in chapter 1, we frame the spread of stress on a network as a Continuous Time Markov Chain (CTMC). It is possible to define the state space as $X_1, X_2, \ldots, X_N$, with $X_i \in \{A, I, E\}$ the state of node i, and to specify all possible transitions between states. Unfortunately, this state space size scales as 3^N where N is the number of individuals in the network. This results in a high dimensional system of ODEs, which is undesirable when we use a numerical method to solve the system. Therefore, we need a different state space which results in a lower dimensional system of ODEs. We use the effective degree approach to look at the dynamics of nodes in a certain state as well as their neighbor's state, as in [32].

We denote the fraction of nodes in state A with a active neighbors, i internally failed neighbors and e externally failed neighbors by $A(a, i, e)$. Similarly, we denote the fraction of nodes in state I and E with a active neighbors, i internally failed neighbors and e externally failed neighbors by $I(a, i, e)$ and $E(a, i, e)$ respectively. For example, the statement $A(4, 1, 0) = \frac{1}{2}$ means that precisely $N/2$ of the N nodes satisfy the condition of being:

> active with 4 active, 1 internally failed and 0 externally failed neighbor(s).

For notational convenience, we denote the fraction of nodes in state $X \in \{A, I, E\}$ with a active neighbors, i internally failed neighbors and e externally failed neighbors by $X(a, i, e)$ Recall that the CTMC is defined on a continuous time scale $t \in [0, \infty)$, but the states $X(a, i, e)$ are discrete random variables, i.e.

$$X(a, i, e) \in \left[0, \frac{1}{N}, \frac{2}{N}, \ldots, 1\right]. \tag{2.1}$$

This aggregation of the state space is based on the assumption that the active neighbors of any active central node are interchangeable, and, similarly, active neighbors of any internally or externally failed central node are interchangeable[15]. Now, the size of the state space is of order $(k_{\max})^3$, where $k_{\max}$ is the maximum degree of the network. From the definition of the states directly follows the fraction of nodes in states A, I and E in equations (2.2a) to (2.2c) respectively.

$$A := \sum_{a=0}^{k_{max}} \sum_{i=0}^{k_{max}} \sum_{e=0}^{k_{max}} A(a, i, e) \tag{2.2a}$$

$$I := \sum_{a=0}^{k_{max}} \sum_{i=0}^{k_{max}} \sum_{e=0}^{k_{max}} I(a, i, e) \tag{2.2b}$$

$$E := \sum_{a=0}^{k_{max}} \sum_{i=0}^{k_{max}} \sum_{e=0}^{k_{max}} E(a, i, e) \tag{2.2c}$$

We aim to derive all possible transitions between different states of the model so that we can represent the model as a system of ODEs. Note that we assume that nodes cannot move directly from internally (externally) failed to externally (internally) failed without passing through the active state.

Next, we will describe all possible transitions between states. We will consider state X(a,i,e) the "center node". Transitions involving the center node are either state transitions of the center node itself or state transitions of neighbors of this center node. For the neighbors of the center node we have four options: (i) an active neighbor fails internally at rate p, (ii) an active neighbor fails externally at rate r if its neighborhood is damaged, (iii) an internally failed neighbor recovers at rate γ_I, (iv) an externally failed neighbor recovers at rate γ_E. Also, the state of the center node itself can change. When the center node is active it has the possibility to internally or externally fail, and when the center node is failed it has the possibility to recover. Figure 2.1 shows the state space, possible transitions are indicated by arrows.

Recall from chapter 1 that $\Theta(m-a)$ equals one when a node has a damaged neighborhood. Furthermore, W_X is defined as the ratio between the number of active neighbors of a node in state X that can fail externally (i.e. have a damaged neighborhood) and the number of active neighbors of nodes in state X. This is defined formally for active, internally failed and externally failed center nodes in equations (2.3a) to (2.3c) respectively.

$$W_A = \frac{\sum_{a=0}^{m}\sum_{i=0}^{k_{max}}\sum_{e=0}^{k_{max}} aA(a,i,e)}{\sum_{a=0}^{k_{max}}\sum_{i=0}^{k_{max}}\sum_{e=0}^{k_{max}} aA(a,i,e)} \tag{2.3a}$$

$$W_I = \frac{\sum_{a=0}^{m}\sum_{i=0}^{k_{max}}\sum_{e=0}^{k_{max}} iA(a,i,e)}{\sum_{a=0}^{k_{max}}\sum_{i=0}^{k_{max}}\sum_{e=0}^{k_{max}} iA(a,i,e)} \tag{2.3b}$$

$$W_E = \frac{\sum_{a=0}^{m}\sum_{i=0}^{k_{max}}\sum_{e=0}^{k_{max}} eA(a,i,e)}{\sum_{a=0}^{k_{max}}\sum_{i=0}^{k_{max}}\sum_{e=0}^{k_{max}} eA(a,i,e)} \tag{2.3c}$$

Note that the definitions in equations (2.3a) to (2.3c) assume that the rate at which any active neighbor of a center node fails externally is the same for any other active neighbor node of this center node. We proceed with an illustration to make the definitions in equations (2.3a) to (2.3c) clearer.

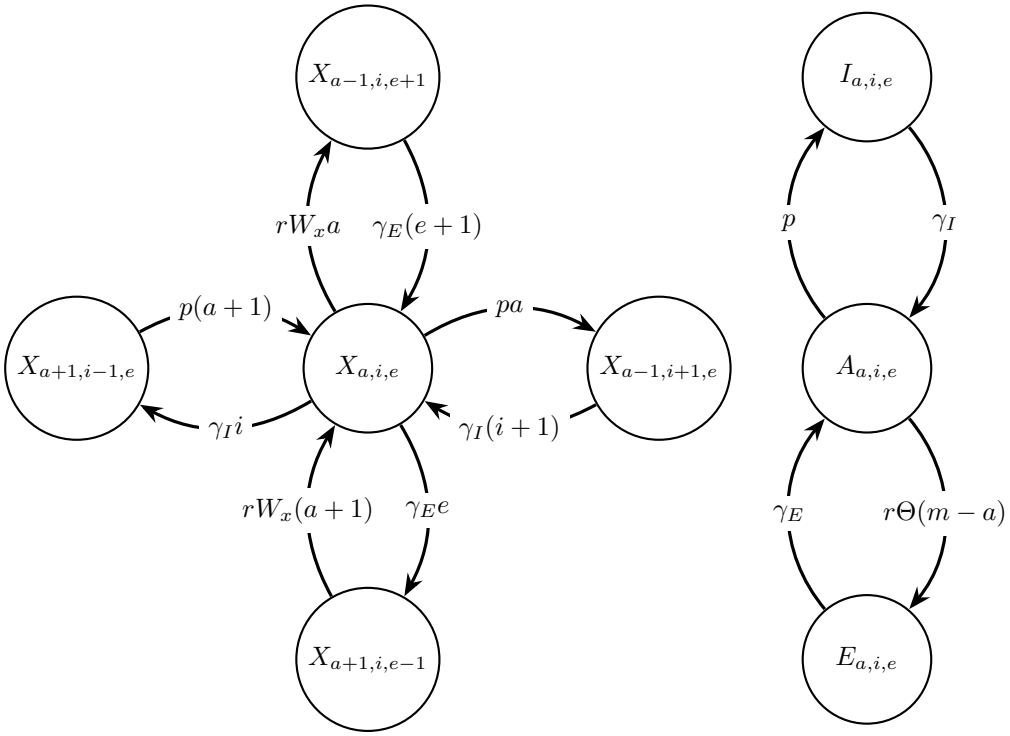

Figure 2.1: Left: Possible state transitions of neighbors of center node $X(a,i,e)$. Right: Possible state transition of center node $X(a,i,e)$. For the sake of readability we denote the state variable $X(a,i,e)$ by $X_{a,i,e}$.

Example 1 (Illustration W_X)**.** *We consider the ten-node network in figure 2.2 where the nodes are only in states A and I, colored black and red respectively. We set $m = 2$, so nodes x_1, x_2 and x_6 have damaged neighborhoods, they are marked with a star. From the network we obtain the states in equation* (2.4)*.*

$$A(1,3,0) = \frac{1}{10} \qquad A(1,2,0) = \frac{1}{10} \qquad A(4,2,0) = \frac{1}{10} \qquad A(3,0,0) = \frac{1}{5} \qquad A(2,0,0) = \frac{1}{10} \tag{2.4}$$

For example, in equation (2.4) $A(1,3,0) = \frac{1}{10}$ *corresponds to node x_1. It is the only node with 1 active and 3 internally failed neighbors. We substitute the states from equation* (2.4) *in equation* (2.3a) *and obtain the following.*

$$W_A = \frac{1 \cdot \frac{1}{10} + 1 \cdot \frac{1}{10} + 2 \cdot \frac{1}{10}}{1 \cdot \frac{1}{10} + 1 \cdot \frac{1}{10} + 4 \cdot \frac{1}{10} + 3 \cdot \frac{1}{5} + 2 \cdot \frac{1}{10}} = \frac{2}{7} \tag{2.5}$$

Note that W_A is equal to the fraction of edges connecting two active nodes in which one of the nodes has a damaged neighborhood. In figure 2.2, 14 edges connect two active nodes, where we also count double-edges. Out of these 14 edges, 4 edges connect an active node with a healthy neighborhood with an active node with a damaged neighborhood, i.e. edges (x_3, x_1), (x_3, x_2), (x_6, x_4) and (x_6, x_5). We conclude that the rate at which active neighbors of active nodes fail is proportional to $\frac{2}{7}$.

Next, we substitute the states from equation (2.4) *in equation* (2.3b) *and obtain the following.*

$$W_I = \frac{3 \cdot \frac{1}{10} + 2 \cdot \frac{1}{10} + 0 \cdot \frac{1}{10}}{3 \cdot \frac{1}{10} + 2 \cdot \frac{1}{10} + 2 \cdot \frac{1}{10} + 0 \cdot \frac{1}{5} + 0 \cdot \frac{1}{10}} = \frac{5}{7} \tag{2.6}$$

From figure 2.2 we see that the number of edges connecting an active node with an internally failed node equals 7. Out of these edges there are indeed 5 edges connecting an inactive neighbor with an active neighbor with a damaged neighborhood. We conclude that the rate at which active neighbors of inactive nodes fail is proportional to $\frac{5}{7}$.

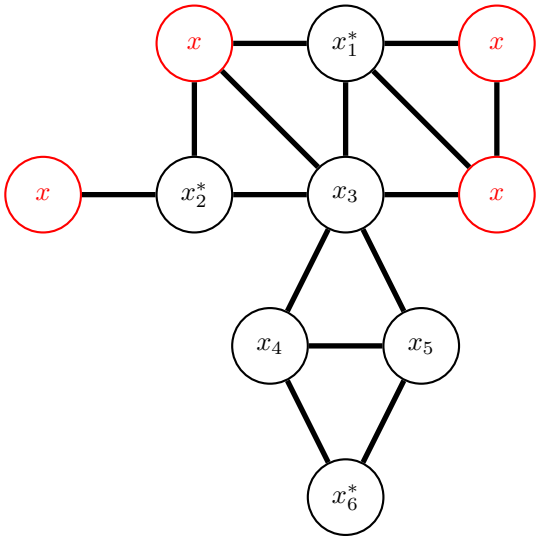

Figure 2.2: Example of a network to illustrate W_X for $X \in [A, I]$, active nodes are colored black and internally failed nodes are colored red. The active nodes are numbered, also, the active nodes with a damaged neighborhood are marked with a star.

2.2 ODEs

Since all transitions are specified, we are able to write the system of ordinary differential equations (ODEs) that describes the change in the number of active, internally failed and externally failed nodes. We will use this systems of ODEs to evaluate the dynamics in the system. To be more specific, in section 2.3 we will derive mean field equations from this system of ODEs and in section 2.4 we will find numerical solutions of the system of ODEs using a Runge-Kutta method.

The total change in $X(a,i,e)$ equals the incoming rates minus the outgoing rates, see figure 2.1. For the fraction of active nodes with a active, i internally failed and e externally failed neighbors we obtain the following equation.

$$\begin{aligned}\frac{d}{dt}A(a,i,e) =& \gamma_I I(a,i,e) + \gamma_E E(a,i,e) - pA(a,i,e) - r\Theta(m-a)A(a,i,e) \\ &+ p\big[(a+1)A(a+1,i-1,e) - aA(a,i,e)\big] \\ &+ \gamma_I\big[(i+1)A(a-1,i+1,e) - iA(a,i,e)\big] \\ &+ rW_A\big[(a+1)A(a+1,i,e-1) - aA(a,i,e)\big] \\ &+ \gamma_E\big[(e+1)A(a-1,i,e+1) - eA(a,i,e)\big]\end{aligned} \tag{2.7}$$

The lines of equation (2.7) correspond respectively to the state transition of the center node, internal failure of an active neighbor of the center node, internal recovery of an internally failed neighbor of the center node, external failure of an active neighbor of the center node and external recovery of an externally failed neighbor of the center node.

The equation for the fraction of internally failed nodes and externally failed nodes are obtained in similar way, resulting in equation (2.8) and equation (2.9) respectively.

$$\begin{aligned}\frac{d}{dt}I(a,i,e) =& pA(a,i,e) - \gamma_I I(a,i,e) \\ &+ p\big[(a+1)I(a+1,i-1,e) - aI(a,i,e)\big] \\ &+ \gamma_I\big[(i+1)I(a-1,i+1,e) - iI(a,i,e)\big] \\ &+ rW_A\big[(a+1)I(a+1,i,e-1) - aI(a,i,e)\big] \\ &+ \gamma_E\big[(e+1)I(a-1,i,e+1) - eI(a,i,e)\big]\end{aligned} \tag{2.8}$$

$$\begin{aligned}\frac{d}{dt}E(a,i,e) =& r\Theta(m-a)A(a,i,e) - \gamma_E E(a,i,e) \\ &+ p\big[(a+1)E(a+1,i-1,e) - aE(a,i,e)\big] \\ &+ \gamma_I\big[(i+1)E(a-1,i+1,e) - iE(a,i,e)\big] \\ &+ rW_A\big[(a+1)E(a+1,i,e-1) - aE(a,i,e)\big] \\ &+ \gamma_E\big[(e+1)E(a-1,i,e+1) - eE(a,i,e)\big]\end{aligned} \tag{2.9}$$

Equations (2.7) to (2.9) are also called master equations[11, 15, 17]. Note that on the border of the state space we have either $a = 0, i = 0$ or $e = 0$, resulting in a closed system. This closed system of deterministic equations can be numerically solved by using standard methods, which we will do in section 2.4 using a Runge-Kutta method.

2.3 Mean field equations

We continue with a mean field approximation of equations (2.7) to (2.9) to investigate the qualitative behavior of the system. Mean-field theories are typically derived under a number of assumptions, the most important of which (for the current discussion) is the assumed lack of dynamic correlations[11]. Under this assumption, nodes fail externally based on a rate that is determined by the overall fraction of active nodes across the network. In particular, the probability that a node has a damaged neighborhood does not depend on his closest neighbors: the assumption leads to no correlation between the state of a node and the state of its neighbors.

Nevertheless, mean field equations are a useful tool: (i) they give a good qualitative description of the process, (ii) they allow to find analytically the behavior of relevant magnitudes such as the fraction of active nodes, (iii) they allow us to study the stability of fixed points[32].

2.3.1 Derivation

Before we start the derivation of the mean field equations from the system of ODEs, as in equations (2.7) to (2.9), we state the following lemma.

Lemma 1. *For $a, i, e \in \mathbb{N}$ such that $a + i + e \in [0, k_{max}]$*

$$\sum_{a=0}^{k_{max}} \sum_{i=0}^{k_{max}} \sum_{e=0}^{k_{max}} \big((a+1)X(a+1, i-1, e) - aX(a, i, e)\big) = 0.$$

Proof. First we change the order of the summations and split the summation into two parts. Additionally, we change the indices of the summation such that the terms inside both summations coincide. We obtain the following.

$$\sum_{e=0}^{k_{max}} \left(\sum_{a=1}^{k_{max}+1} \sum_{i=-1}^{k_{max}-1} aX(a, i, e) - \sum_{a=0}^{k_{max}} \sum_{i=0}^{k_{max}} aX(a, i, e) \right) = 0$$

Since k_{max} is the maximal degree of a node it is not possible to have $k_{max} + 1$ active neighbors. This gives $X(k_{max}+1, i, e) = 0$ for all i and e. The same holds for $i = -1$: it is not possible to have a negative number of neighbors. Therefore $X(a, -1, e) = 0$ for all a and e. We obtain the following.

$$\sum_{e=0}^{k_{max}} \left(\sum_{a=1}^{k_{max}} \sum_{i=0}^{k_{max}-1} aX(a, i, e) - \sum_{a=0}^{k_{max}} \sum_{i=0}^{k_{max}} aX(a, i, e) \right) = 0$$

Next, in the first summation inside the brackets we add and substract the term for $i = k_{max}$, and in the second summation inside the brackets we add and subtract the term for $a = 0$. This leads to the following.

$$\sum_{e=0}^{k_{max}} \left(\left(\sum_{a=1}^{k_{max}} \sum_{i=0}^{k_{max}} aX(a, i, e) - \sum_{a=1}^{k_{max}} aX(a, k_{max}, e) \right) - \left(\sum_{i=0}^{k_{max}} 0 \cdot X(0, i, e) + \sum_{a=1}^{k_{max}} \sum_{i=0}^{k_{max}} aX(a, i, e) \right) \right) = 0$$

Firstly, the first term and the fourth term are the same: as the fourth term is subtracted from the first they cancel out. Secondly, because $a + i + e \leq k_{max}$ we have $X(a, k_{max}, e) = 0$ for $a \geq 1$, so the second summation also equals 0. And lastly, it can easily be seen that the third term equals zero. This concludes the lemma. Note that similar lemmas hold for permutations of a, i, e. □

Next, we derive the mean field equations by summing equations (2.7) to (2.9) over all degrees a, i, e. Applying lemma 1 makes sure a lot of terms cancel out. We obtain the following set of mean field equations, recall from chapter 1 that A, I and E represent the average fraction of active, internally failed and externally failed nodes respectively.

$$\frac{dA}{dt} = \gamma_I I + \gamma_E E - pA - r \sum_{a=0}^{m} \sum_{i=0}^{k_{max}} \sum_{e=0}^{k_{max}} A(a, i, e) \tag{2.10a}$$

$$\frac{dI}{dt} = pA - \gamma_I I \tag{2.10b}$$

$$\frac{dE}{dt} = r \sum_{a=0}^{m} \sum_{i=0}^{k_{max}} \sum_{e=0}^{k_{max}} A(a, i, e) - \gamma_E E \tag{2.10c}$$

We continue with a second lemma that gives a mean field approximation for the fraction of active nodes with a damaged neighborhood.

Lemma 2. *For a network with arbitrary degree distribution $f(k)$ we obtain the following mean field approximation.*

$$\sum_{a=0}^{m} \sum_{i=0}^{k_{max}} \sum_{e=0}^{k_{max}} A(a, i, e) = A \sum_{k} f(k) \sum_{j=0}^{m} \binom{k}{j} (1-A)^{k-j} A^j$$

Proof. We aim to find an approximation for the fraction of active nodes with a damaged neighborhood. This can be found by multiplying the expected fraction of active nodes by the probability that an active node has a damaged neighborhood.

The probability that a random node of degree k has j active neighbors can be approximated as follows.

$$P(\text{node of degree } k \text{ has } j \text{ active neighbors}) = \binom{k}{j} (1-A)^{k-j} A^j \tag{2.11}$$

A node has a damaged neighborhood when it has less than or equal to m active neighbors, so if we sum the probability of equation (2.11) over $j \in [0, m]$ and over the degree distribution k we derive the probability that an active node has a damaged neighborhood. We obtain the following.

$$P(\text{active node has a damaged neighborhood}) = \sum_k f(k) \sum_{j=0}^{m} \binom{k}{j} (1-A)^{k-j} A^j \tag{2.12}$$

Note that in equation (2.12) we assume that the degree of all nodes is at least m. The expected number of active nodes in the network is A, so if we multiply equation (2.12) by A we obtain the mean field approximation stated in lemma 2. □

Substituting the approximation of lemma 2 in equations (2.10a) to (2.10c) gives the following system of mean-field equations.

$$\frac{dA}{dt} = \gamma_I I + \gamma_E E - pA - rA \sum_k f(k) \sum_{j=0}^{m} \binom{k}{j} (1-A)^{k-j} A^j \tag{2.13a}$$

$$\frac{dI}{dt} = pA - \gamma_I I \tag{2.13b}$$

$$\frac{dE}{dt} = rA \sum_k f(k) \sum_{j=0}^{m} \binom{k}{j} (1-A)^{k-j} A^j - \gamma_E E \tag{2.13c}$$

2.3.2 Analysis

Now that we derived the system of mean field equations we will find fixed points of the system and investigate their stability. Since $A + I + E = 1$ we only consider equations (2.13a) and (2.13b) and use the substitution $E = 1 - A - I$, this leads to a system of two differential equations in two unknown as follows.

$$\frac{dA}{dt} = \gamma_I I + \gamma_E (1 - A - I) - pA - rA \sum_k f(k) \sum_{j=0}^{m} \binom{k}{j} (1-A)^{k-j} A^j \tag{2.14a}$$

$$\frac{dI}{dt} = pA - \gamma_I I \tag{2.14b}$$

From this system follows the steady state solution for I as follows.

$$\bar{I} = \frac{p}{\gamma_I} A \tag{2.15}$$

Next, we substitute this steady state solution in equation (2.14a). We obtain the following.

$$\frac{dA}{dt} = \gamma_I \left(\frac{p}{\gamma_I} A \right) + \gamma_E \left(1 - A - \frac{p}{\gamma_I} A \right) - pA - rA \sum_k f(k) \sum_{j=0}^{m} \binom{m}{j} (1-A)^{k-j} A^j \tag{2.16}$$

From this follows the equation that is satisfied in the steady state as follows.

$$0 = \gamma_E \left(1 - A - \frac{p}{\gamma_I} A \right) - rA \sum_k f(k) \sum_{j=0}^{m} \binom{m}{j} (1-A)^{k-j} A^j \qquad \Longleftrightarrow$$

$$A = 1 - \frac{p}{\gamma_I} A - \frac{r}{\gamma_E} A \sum_k f(k) \sum_{j=0}^{m} \binom{m}{j} (1-A)^{k-j} A^j \tag{2.17}$$

To summarize, with equation (2.17) we found an expression for the number of active nodes that is satisfied in the equilibrium. We observe that equation (2.17) only depends on the combination of parameter values $\frac{p}{\gamma_I}$ and $\frac{r}{\gamma_E}$. Therefore, in what follows, we fix the recovery rates γ_I and γ_E and investigate the dynamics in the model when varying failure rates p and r. Recall from chapter 1 we use the more convenient parameter p^*, for a derivation see appendix A.1. The parameter p^* corresponds to the fraction of internally failed nodes in the network.

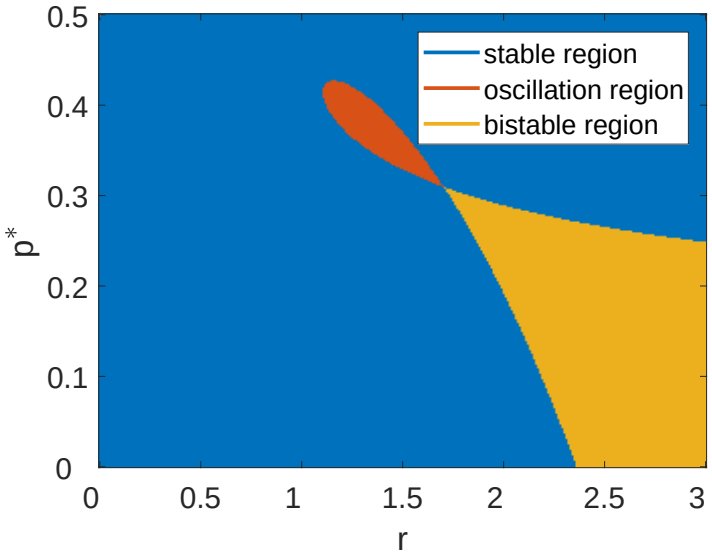

Figure 2.3: For a regular network with $\bar{k} = 10, m = 4$ and parameter values $\gamma_I = 0.01, \gamma_E = 1$. Phase diagram in the (r, p^*)-plane.

For fixed parameter values p^*, r, γ_I and γ_E we are able to find the stable solutions of equation (2.17). We investigate the stability of these fixed points by linearizing equations (2.14a) and (2.14b) around the fixed points.

Suppose $(\bar{A}, \bar{I})$ is a fixed point of the system $(f(A, I), g(A, I)) := (\frac{dA}{dt}, \frac{dI}{dt})$. The linearized system is given by

$$\begin{pmatrix} \dot{u} \\ \dot{v} \end{pmatrix} = J \begin{pmatrix} u \\ v \end{pmatrix}, \qquad \text{with} \qquad J = \begin{pmatrix} \frac{df}{dA}(\tilde{A}, \tilde{I}) & \frac{df}{dI}(\tilde{A}, \tilde{I}) \\ \frac{dg}{dA}(\tilde{A}, \tilde{I}) & \frac{dg}{dI}(\tilde{A}, \tilde{I}) \end{pmatrix}. \tag{2.18}$$

Here we defined $u = A - \bar{A}$ and $v = I - \bar{I}$. From equations (2.13a) and (2.13b) we obtain the Jacobian

$$J = \begin{pmatrix} -\gamma_E - p - r\mathbf{s}(\bar{A}) & \gamma_I - \gamma_E \\ p & -\gamma_I \end{pmatrix}, \tag{2.19}$$

with

$$\mathbf{s}(A) = \sum_k f_k \sum_j \binom{k}{j} \big((j+1)A^j(1-A)^{k-j} - (k-j)(1-A)^{k-j-1}A^{j+1}\big). \tag{2.20}$$

Now we can substitute the steady state solutions $(\tilde{A}, \tilde{I})$ in J and calculate the eigenvalues of the matrix to determine the stability of $(\tilde{A}, \tilde{I})$. If the eigenvalues have negative real parts, we conclude that the solution is stable. Figure 2.3 shows the phase diagram, it consist of three regions. The stable region corresponds to the parameter values where only one stable solution is found. The oscillatory region corresponds to the parameter values where one or three unstable solutions are found. The bistable region corresponds to the parameter values where two stable solutions and one unstable solution are found.

Next, we illustrate the behavior in the different regions of the phase diagram by looking at cross-sections for fixed values of r. Figures 2.4a to 2.4c shows, for three values of r, the steady states of the fraction of active nodes versus p^*. We have the following cases for the behavior of the system.

(i) Stable behavior: the system has only one globally stable equilibrium. This is the case for $r = 1$ and for all p^* in figure 2.4a.

(ii) Oscillatory behavior: the system has one unstable equilibrium. This is the case for $r = 1.5$ for some values of p^*, the system switches between states. Inside the oscillatory region of the phase diagram in figure 2.3 the closed system has only one unstable solution, so we obtain a limit cycle in the phase space.

(iii) Bistable behavior: the system has two stable equilibria and one unstable equilibrium. This is the case for $r = 2$ for some values of p^*. It depends on the initial conditions of the system which stable state is reached.

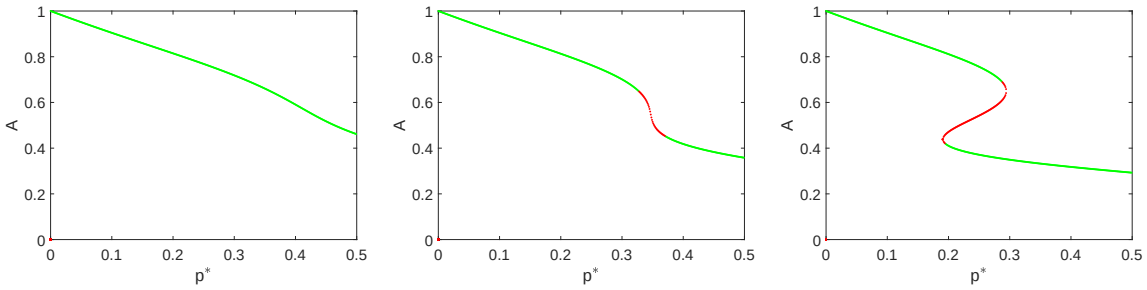

(a) $r = 1$ (b) $r = 1.5$ (c) $r = 2$

Figure 2.4: Steady states of A versus p^* for different values of r for a regular network with $\bar{k} = 10, m = 4$ and parameter values $\gamma_I = 0.01, \gamma_E = 1$. Green lines correspond to stable solutions and red lines correspond to unstable solutions. (a) For $r = 1$ we find one stable solution for every value of p^*. (b) For $r = 1.5$ we again find one solution for every value of p^*, but some of them are unstable. This means that for this rate p^* the system is unstable and shows oscillatory behavior. (c) For $r = 2$ there is a region of parameter values for p^* where the system has three equilibria, two stable and one unstable.

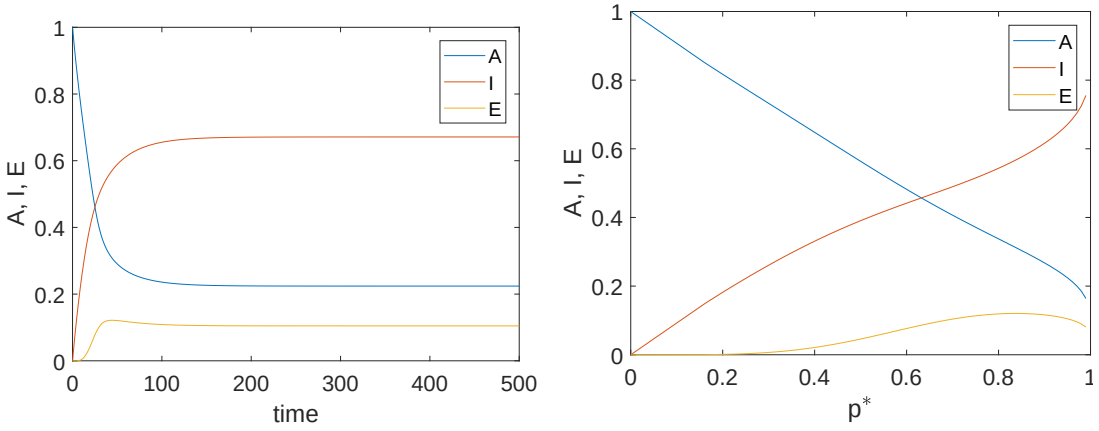

(a) (b)

Figure 2.5: For a regular network with $\bar{k} = 10, m = 4$ and parameter values in the stable region: $r = 0.5, \gamma_I = 0.01, \gamma_E = 1$ and initial condition $A = 1$. (a) Time evolution of the fraction of active nodes (A), internally failed nodes (I) and externally failed nodes (E) obtained by solving equations (2.7) to (2.9) for $p^* = 0.95$ with the Runge-Kutta method. (b) The stable solutions of A, I, E versus p^*, the system shows stable behavior.

2.4 Numerical solution

In this section we will use the Runge-Kutta method to numerically solve equations (2.7) to (2.9) for different combination of parameter values (r, p^*).

First, we will investigate the behavior of the system for parameter values in the stable region. We solve equations (2.7) to (2.9) for parameter values $(r, p^*) = (0.5, 0.95)$ and initially all nodes active, i.e. $A = 1$. Figure 2.5a shows the evolution of the density of active, internally failed and externally failed nodes for a regular network with $\bar{k} = 10$ and threshold $m = 4$. We observe that the initial behavior of the system depends on its initial values, but eventually it reaches a steady state independent of its initial values.

We continue by finding stable solutions of the system for $r = 0.5$ for $p^* \in [0, 1]$. Figure 2.5b shows the stable density of active, internally failed and externally failed nodes versus p^*. Here, the stable solutions are independent of the initial value. This means that, if we initially take all nodes as internally failed $(I = 1)$, the system shows different behavior initially but eventually reaches the same stable equilibrium. We conclude that for these parameter values the behavior of the system is independent of its initial state, also, we do not observe a phase transition.

We repeat the procedure for $r = 3$, see figure 2.6, and find that the system undergoes a first order phase transition for $p_c^* = 0.41$, the system changes its stable state from high-active to low-active. The fraction of externally failed nodes rises critically at $p^* = 0.41$. This can be understood intuitively: from

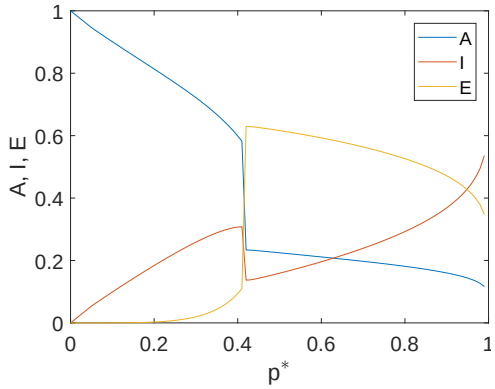

Figure 2.6: For a regular network with $\bar{k} = 10, m = 4$ and parameter values $r = 3, \gamma_I = 0.01, \gamma_E = 1$. The stable solutions of A, I, E versus p^*. For $p_c^* = 0.41$ the system shows a first order phase transition where the stable state of the system switches from high-active to low-active.

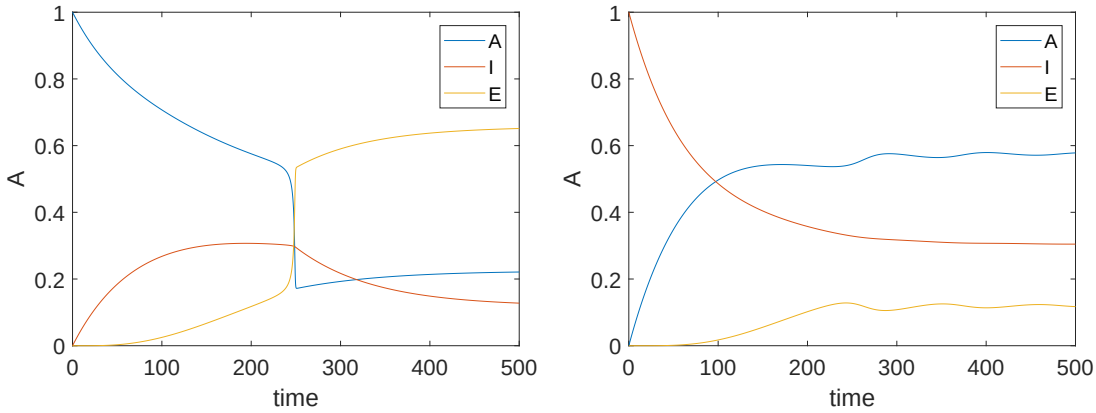

(a) (b)

Figure 2.7: For a regular network with $\bar{k} = 10, m = 4$ and parameter values $r = 3.2, p^* = 0.41, \gamma_I = 0.01, \gamma_E = 1$. Time evolution of the fraction of active, internally failed and externally failed nodes A for initial conditions (a) $A = 1$ and (b) $I = 1$. The stable state of the system depends on the initial condition.

the definition of p^* in equation (A.4) we expect that for $p^* = 0.4$ the system has a fraction of 0.4 inactive nodes. Since the threshold for the activity of the neighborhood is $m = 4$ for our regular network of degree 10 and as we do not consider local dependencies in our effective degree model, all nodes now are assumed to have a damaged neighborhood. And because external failure happens at higher rate than internal failure, the external failures rise sharply. Additionally, the sudden rise of external failure at p_c^* makes less nodes available for internal failure, explaining the slope decrease of I for $p^* > p_c^*$.

Now we will illustrate the behavior of the system for parameter values in the bistable region. In this region the stable solution of the system depends on its initial value. The time evolution of the fraction of active, internally failed and externally failed nodes obtained by the effective degree approach for $r = 3.2$ and $p^* = 0.41$ is shown in figure 2.7. We observe that the stable state of the system depends on its initial state. When all nodes are active initially, the system converges to a stable equilibrium where the nodes are predominantly failed. On the other hand, when all nodes are internally failed initially, the system converges to an equilibrium where the nodes are predominantly active.

Finally, we investigate the oscillatory behavior of the system. Figure 2.8 shows the time evolution of A by solving equations (2.7) to (2.9) with the Runge-Kutta method for fixed $r = 2$ and different $p^* \in [0, 1)$. The system exhibits a Hopf bifurcation for $p^* \approx 0.47$: the stability in the system switches and a periodic solution arises. We observe that the system exhibits oscillatory behavior for $p^* \in [0.47, 0.55]$. For other values of p^* the system converges to a stable equilibrium.

In figure 2.9 the time evolution is plotted for $p^* = 0.50$. As mentioned in [32], we observe three stages.

(i) Initially all nodes are active and only internal failures occur as the neighborhoods of the majority of the nodes are healthy. Therefore, in this stage A decreases, I increases and E remains near zero.

(ii) Due to the internally failed nodes in stage (i), the predominant part of the nodes now has a damaged neighborhood. This results in external failures rising faster than internal failures. Consequently, in this stage A decreases and both I and E increase, with E increasing at a faster rate. These dynamics are a competition between internal failure and external failure [43], where external failure wins.

(iii) In the next stage the fraction of active nodes increases due to recovery. Because $\gamma_I < \gamma_E$ the externally failed nodes recover faster compared to the internally failed nodes, resulting in a more rapid decrease of externally failed nodes than internally failed. Therefore, in this stage A increases and both I, E decrease, with E decreasing faster. When a local maximum for A and a local minimum for E are reached simultaneously, there are more nodes A available to fail. This again leads to the competitive behavior of internal and external failure of stage (ii).

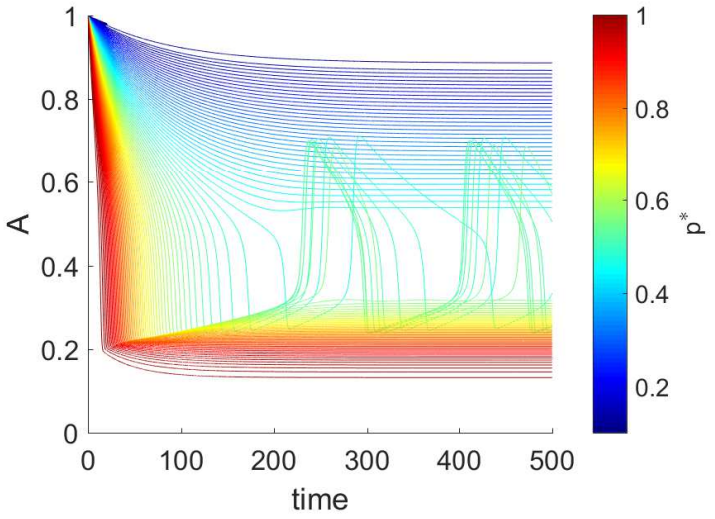

Figure 2.8: For a regular network with $\bar{k} = 10, m = 4$ and parameter values $r = 2, \gamma_I = 0.01, \gamma_E = 1$ and initial condition $A = 1$. Time evolution of the fraction of active nodes A for values of $p^* \in [0, 1)$. The system exhibits oscillatory behavior for $p^* \in [0.47, 0.55]$.

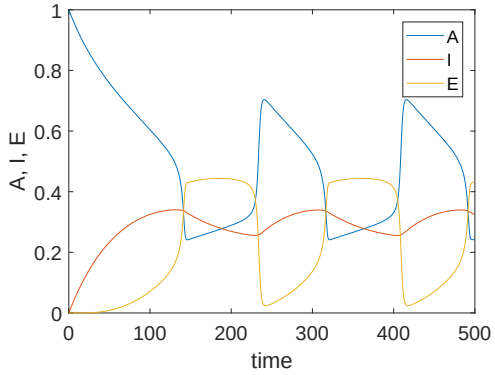

Figure 2.9: For a regular network with $\bar{k} = 10, m = 4$, parameter values $r = 2, \gamma_I = 0.01, \gamma_E = 1$ and initial condition $A = 1$. Time evolution of the fraction of active nodes (A), internally failed nodes (I) and externally failed nodes (E) for $p^* = 0.5$, the parameter value for which the system exhibits oscillatory behavior.

2.5 Extra transition

In this section we will see that including the possibility for externally failed nodes to fail internally leads to different dynamics: the oscillation region vanishes.

In sections 2.3 and 2.4 we have seen competition between internally failed and externally failed nodes. The same model is studied by [19], who uses transition probabilities instead of rates and updates the state of the system successively. Additionally, [19] stipulates a modification of the failures by adding an extra transition to the model, namely the transition from external failure to internal failure. In the context of this thesis, this means that nodes always have the possibility to stop functioning, regardless of their current state. We assumed that internal failure is worse than external failure by setting $\gamma_I < \gamma_E$. Giving externally failed nodes the possibility to fail internally strengthens this assumption. In what follows, we investigate the effect of this extra transition when we frame the model in a CTMC.

In section 2.1 we discussed all possible transitions between states during a time interval of length Δt. Now, two transitions are added: (i) The internal failure of an externally failed neighborhood at rate pa denoted by $X(a,i,e,) \mapsto X(a,i+1,e-1)$ and (ii) the internal failure of an externally failed center node at rate p denoted by $E(a,i,e) \mapsto I(a,i,e)$.

Including these two transitions into equations (2.7) to (2.9) gives the following system of differential equations. The added terms are in bold.

$$\begin{aligned}\frac{d}{dt}A(a,i,e) =& \gamma_I I(a,i,e) + \gamma_E E(a,i,e) - pA(a,i,e) - r\Theta(m-a)A(a,i,e) \\ &+ p\big[(a+1)A(a+1,i-1,e) - aA(a,i,e)\big] \\ &+ \gamma_I\big[(i+1)A(a-1,i+1,e) - iA(a,i,e)\big] \\ &+ rW_A\big[(a+1)A(a+1,i,e-1) - aA(a,i,e)\big] \\ &+ \gamma_E\big[(e+1)A(a-1,i,e+1) - eA(a,i,e)\big] \\ &+ \mathbf{p}\big[(\mathbf{e+1})\mathbf{A}(\mathbf{a},\mathbf{i-1},\mathbf{e+1}) - \mathbf{eA}(\mathbf{a},\mathbf{i},\mathbf{e})\big]\end{aligned} \tag{2.21}$$

$$\begin{aligned}\frac{d}{dt}I(a,i,e) =& pA(a,i,e) - \gamma_I I(a,i,e) + \mathbf{pE}(\mathbf{a},\mathbf{i},\mathbf{e}) \\ &+ p\big[(a+1)I(a+1,i-1,e) - aI(a,i,e)\big] \\ &+ \gamma_I\big[(i+1)I(a-1,i+1,e) - iI(a,i,e)\big] \\ &+ rW_A\big[(a+1)I(a+1,i,e-1) - aI(a,i,e)\big] \\ &+ \gamma_E\big[(e+1)I(a-1,i,e+1) - eI(a,i,e)\big] \\ &+ \mathbf{p}\big[(\mathbf{e+1})\mathbf{I}(\mathbf{a},\mathbf{i-1},\mathbf{e+1}) - \mathbf{eI}(\mathbf{a},\mathbf{i},\mathbf{e})\big]\end{aligned} \tag{2.22}$$

$$\begin{aligned}\frac{d}{dt}E(a,i,e) =& r\Theta(m-a)A(a,i,e) - \gamma_E E(a,i,e) - \mathbf{pE}(\mathbf{a},\mathbf{i},\mathbf{e}) \\ &+ p\big[(a+1)E(a+1,i-1,e) - aE(a,i,e)\big] \\ &+ \gamma_I\big[(i+1)E(a-1,i+1,e) - iE(a,i,e)\big] \\ &+ rW_A\big[(a+1)E(a+1,i,e-1) - aE(a,i,e)\big] \\ &+ \gamma_E\big[(e+1)E(a-1,i,e+1) - eE(a,i,e)\big] \\ &+ \mathbf{p}\big[(\mathbf{e+1})\mathbf{E}(\mathbf{a},\mathbf{i-1},\mathbf{e+1}) - \mathbf{eE}(\mathbf{a},\mathbf{i},\mathbf{e})\big]\end{aligned} \tag{2.23}$$

If we now sum equations (2.21) to (2.23) over all degrees of a, i, e and apply lemma 2 we obtain the following set of mean field equations. The added terms are in bold.

$$\frac{dA}{dt} = \gamma_I I + \gamma_E E - pA - rA\sum_k f(k)\sum_{j=0}^{m}\binom{k}{j}(1-A)^{k-j}A^j \tag{2.24a}$$

$$\frac{dI}{dt} = pA - \gamma_I I + \mathbf{pE} \tag{2.24b}$$

$$\frac{dE}{dt} = rA\sum_k f(k)\sum_{j=0}^{m}\binom{k}{j}(1-A)^{k-j}A^j - \gamma_E E - \mathbf{pE} \tag{2.24c}$$

Substituting $E = 1 - A - I$ in equation (2.24b) results in the following steady state solution.

$$I = \frac{p}{p+\gamma_I}$$

Substituting this steady state solution in equation (2.24a) and using that $E = 1 - A - I$ gives the

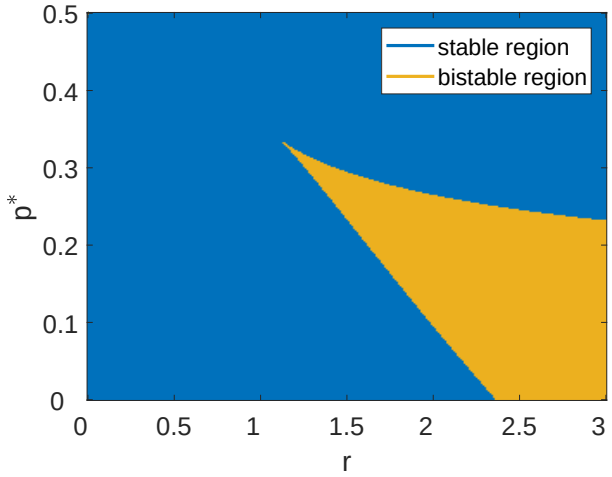

Figure 2.10: For a regular network, with $\bar{k} = 10$, $m = 4$ and parameter values $\gamma_I = 0.01, \gamma_E = 1$. Phase diagram in the (r, p^*)-plane.

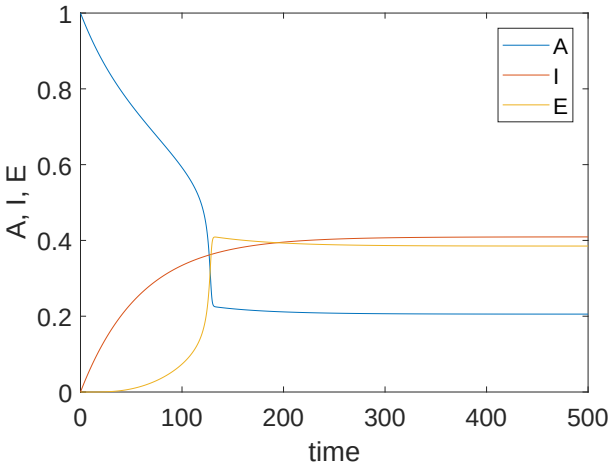

Figure 2.11: For a regular network with $\bar{k} = 10, m = 4$, parameter values $r = 2, \gamma_I = 0.01, \gamma_E = 1$ and initial condition $A = 1$. Time evolution of the fraction of active nodes (A), internally failed nodes (I) and externally failed nodes (E) for $p^* = 0.5$. By adding the extra transition from externally failed to internally failed the system exhibits no oscillatory behavior.

following equation in A that is satisfied in the steady state.

$$0 = \gamma_I \frac{p}{p+\gamma_I} + \gamma_E(1 - A - \frac{p}{p+\gamma_I}) - pA - rA\sum_k f(k)\sum_{j=0}^{m}\binom{k}{j}(1-A)^{k-j}A^j \tag{2.25}$$

For all values of (r, p^*) we can find fixed points of equation (2.25) and we can linearize the system at the fixed point to investigate their stability. Figure 2.10 shows the phase diagram where we indicate the different regions. We conclude that by including the extra transition the oscillatory region vanishes. This can be intuitively understood: by adding the transition from externally failed to internally failed the competition between internally failed and externally failed disappears; now nodes always have the possibility to fail internally.

To illustrate our findings, we solve equations (2.21) to (2.23) with a Runge-Kutta method for the same parameter values used in figure 2.9, where the system exhibited oscillatory behavior. The time evolution of the fraction of active, internally failed and externally failed nodes is shown in figure 2.11. We observe that the system initially shows similar behavior as the system without the transition, but eventually reaches a stable equilibrium.

To summarize: by adding the possibility for externally failed nodes to fail internally the oscillatory behavior vanishes. This is explained by the fact that internal failure always wins from external failure, resulting in the disappearance of the limit cycle.

Chapter 3

Interconnected networks

In this chapter we will consider the failure-recovery model for interconnected networks, where two networks are coupled so that the nodes in the different networks depend on each other. So instead of only taking into account the internal and external failure of a node, we also consider dependency failure.

In this thesis, we will not investigate the robustness of different interconnected networks. But, we aim to introduce the interconnected networks and explore the qualitative behavior of the system.

We will start with an introduction about interconnected networks and introduce the failure-recovery model for the interconnected networks. Subsequently, similar to chapter 2, we will use the effective degree approach to analytically study the model.

3.1 Introduction and model introduction

Lots of research on cascading failures has been only concentrated on the case of a single network, ignoring that many real-world networks interact with and depend on each other to provide proper functionality[34]. An example of such system is the traffic flow between cities, through the sea port and airport networks in which the flow of individuals or goods in a city decays if it does not receive traffic from one of these networks[33]. A fundamental property of interconnected networks is that when nodes in one network fail, they may lead to the failure of dependent nodes in the other network[7]. Thus, the functionality of a network does not only depend on itself, but also on its coupled network. The interdependence between networks has catastrophic effects on their robustness, i.e., node failure in one network may trigger the failure of dependent nodes in other networks which may produce an iterative cascade of failures in several interdependent networks, leading to a global cascade of failures[34].

3.1.1 Networks

Networks can have different topologies and bidirectional interdependency links between two networks can be formed in different ways. We list some of the possible couplings.

(a) One-to-one random coupling: each node in network A is randomly connected to exactly one node in network B. This type of coupling is studied in [4, 7, 34, 38]. However, in real-world networks, a single node in network A may depend on more than one node in network B and will function as long as one of the support nodes in network B is still connected[30].

(b) Intersimilar coupling: the nodes that are interconnected show some similarity. For example, [5] stipulates a one-to-one correspondence between two networks with the same degree distribution and nodes are coupled according to their degree. Note that this does not imply that two networks with the same topology couple the identical nodes, but only that nodes with (approximately) the same degree are coupled. Note that intersimilarity does not only occur when nodes with similar degree are coupled, but also when neighbors of interdependent nodes also tend to be interdependent[24].

In real-world networks such couplings can be significant. It is highly unlikely that a high degree node has a dependency link with a low degree node in its coupled network[24]. The opposite holds, in real world interacting networks the hubs in one network are more likely to depend on the hubs of another network. For instance, one may expect that a person with many friends in one social network would also have many friends in another social network, being a friendly person[6].

(c) Partial coupling: a fraction of network A nodes depend on a fraction of network B nodes, this coupling is studied in [8].

(d) Layered coupling: the two networks include the same nodes and a dependency link is formed between the same nodes in network A and B. Within the networks the link represent a different connection for every network. We can think of a layered network model for the transportation system where the nodes represent cities and the links between nodes represent connections between these cities. Here each layer represents a kind of transportation medium (e.g. airlines, railways, roads, etc.), interdependency links are formed between the same cities. This type of networks is studied in [6, 13].

3.1.2 Model introduction

In this section we will introduce the failure-recovery model for the interconnected networks. We frame the spread of stress on the interconnected networks as a Continuous Time Markov Chain (CTMC). Similar to the single network, the dynamic behavior consist of the events *failure* and *recovery*. Since now we deal with two interconnected networks, we also consider dependency failure. Four fundamental assumptions are as follows.

(i) A node in network A (B) fails independently of other nodes at rate p_A (p_B), this type of failure is referred to as *internal failure*.

(ii) A node in network A (B) fails at rate r_A (r_B) if his neighborhood is damaged, the neighborhood of a node is damaged when it has less than or equal to m active neighbors within its own network. This type of failure is referred to as *external failure*.

(iii) A node fails with probability r_D if its dependent node in the other network fails. This type of failure is referred to as *dependency failure*.

(iv) Nodes recover from failure at rates γ_I, γ_E and γ_D from respectively internal, external and dependency failure.

Note that in (iii) we assume that nodes have maximally one dependency link to the other network. We denote the fraction of active, internally failed, externally failed and dependency failed nodes in network A by A^A, I^A, E^A and D^A respectively. Replacing the superscript A by B gives the fractions for network B.

The failure-recovery model for interconnected networks is also used in [19, 38]. In [38] it is assumed that dependency failure is determinstic, meaning that if a node fails its counterpart in the connected networks also fails. In [19] it is assumed that dependency failure is probabilistic, meaning that if a node fails its counterpart fails with some probability.

Similar to chapter 2 we assume that nodes recover from internal and external failure at rate $\gamma_I = 0.01$ and $\gamma_E = 1$ respectively. As in [20], we assume that recovery from dependency failure happens at the same rate as external failure, i.e. $\gamma_D = 1$.

3.2 Effective degree approach

We use the effective degree approach to look at the dynamics of nodes in the interconnected networks in a certain state as well as the state of their neighbors. The approach is similar to the approach in chapter 2, but now nodes can also be in state D if they are failed due to dependency failure. In the following, we consider two regular networks of equal size N. We assume the networks are coupled according to a one-to-one random coupling, so every node has a random dependency link to the other network.

We denote the fraction of nodes in network A in state $X \in \{A, I, E, D\}$ with a active neighbors, i internally failed neighbors, e externally failed neighbors and d dependency failed neighbors within network A by $X^A(a, i, e, d)$. For example, $D^A(3, 5, 2, 0) = 0.1$ means that a fraction 0.1 of the nodes failed due to dependency failure with 3 active, 5 internally failed, 2 externally failed and 0 dependency failed neighbor(s) within their own network.

From the definition of the state directly follows the fraction of nodes in network A in state A^A, I^A, E^A and D^A respectively.

$$A^A := \sum_{a=0}^{k_{max}} \sum_{i=0}^{k_{max}} \sum_{e=0}^{k_{max}} \sum_{d=0}^{k_{max}} A^A(a,i,e,d) \tag{3.1a}$$

$$I^A := \sum_{a=0}^{k_{max}} \sum_{i=0}^{k_{max}} \sum_{e=0}^{k_{max}} \sum_{d=0}^{k_{max}} I^A(a,i,e,d) \tag{3.1b}$$

$$E^A := \sum_{a=0}^{k_{max}} \sum_{i=0}^{k_{max}} \sum_{e=0}^{k_{max}} \sum_{d=0}^{k_{max}} E^A(a,i,e,d) \tag{3.1c}$$

$$D^A := \sum_{a=0}^{k_{max}} \sum_{i=0}^{k_{max}} \sum_{e=0}^{k_{max}} \sum_{d=0}^{k_{max}} D^A(a,i,e,d) \tag{3.1d}$$

By replacing the superscripts A with B in equations (3.1a) to (3.1d) we obtain the fraction of nodes in network B in state A^B, I^B, E^B and D^B respectively.

We aim to derive all possible transitions between different states of the model so that we can represent the model as a system of ODEs. We assume that nodes cannot move directly between the states I, E and D without passing through the active state. All possible transitions of the center node in the interconnected networks are shown in figure 3.1. Here we have for the ratio of external failure within network A the following.

$$W_A^A = \frac{\sum_{a=0}^{m} \sum_{i=0}^{k_{max}} \sum_{e=0}^{k_{max}} \sum_{d=0}^{k_{max}} aA^A(a,i,e,d)}{\sum_{a=0}^{k_{max}} \sum_{i=0}^{k_{max}} \sum_{e=0}^{k_{max}} \sum_{d=0}^{k_{max}} aA^A(a,i,e,d)} \tag{3.2}$$

Similar expression hold for W_I^A, W_E^A and W_D^A.

Note that the rate at which an active center node in network A fails due to dependency failure is proportional to the fraction of inactive nodes in network B, i.e. $\big(1 - A^B\big)$. Also, in figure 3.1, V_X^A is the ratio between the fraction of active neighbors of a node in state X that can fail due to dependency failure and the fraction of neighbor nodes in state X.

3.2.1 ODE

As all transitions are specified, we are able to write down the system of ODEs. We obtain the following equation for the active nodes in network A.

$$\begin{aligned}
\frac{d}{dt}A^A(a,i,e,d) = {} & \gamma_I I^A(a,i,e,d) + \gamma_E E^A(a,i,e,d) - p_A A^A(a,i,e,d) - r_A \Theta(m-a) A^A(a,i,e,d) \\
& + \gamma_D D^A(a,i,e,d) - r_D(1 - A^B) \\
& + p_A\big[(a+1)A^A(a+1,i-1,e,d) - aA^A(a,i,e,d)\big] \\
& + \gamma_I\big[(i+1)A^A(a-1,i+1,e,d) - iA^A(a,i,e,d)\big] \\
& + r_A W_A^A\big[(a+1)A^A(a+1,i,e-1,d) - aA^A(a,i,e,d)\big] \\
& + \gamma_E\big[(e+1)A^A(a-1,i,e+1,d) - eA^A(a,i,e,d)\big] \\
& + r_D V_X^A\big[(a+1)A^A(a+1,i,e,d-1) - aA^A(a,i,e,d)\big] \\
& + \gamma_D\big[(d+1)A^A(a-1,i,e,d+1) - dA^A(a,i,e,d)\big]
\end{aligned} \tag{3.3}$$

Note that equation (3.3) is similar to the one found in equation (2.7) for the single model, except for the addition of the neighbor d to the state and the addition of the extra transitions. To be more specific, in equation (3.3) the second line reflects the new transitions of the center node, and the last two lines reflect the transitions of the neighbor nodes.

The differential equations for the fraction of internally failed, externally failed and dependency failed nodes are obtained in a similar way, resulting in equations (3.4) to (3.6) respectively.

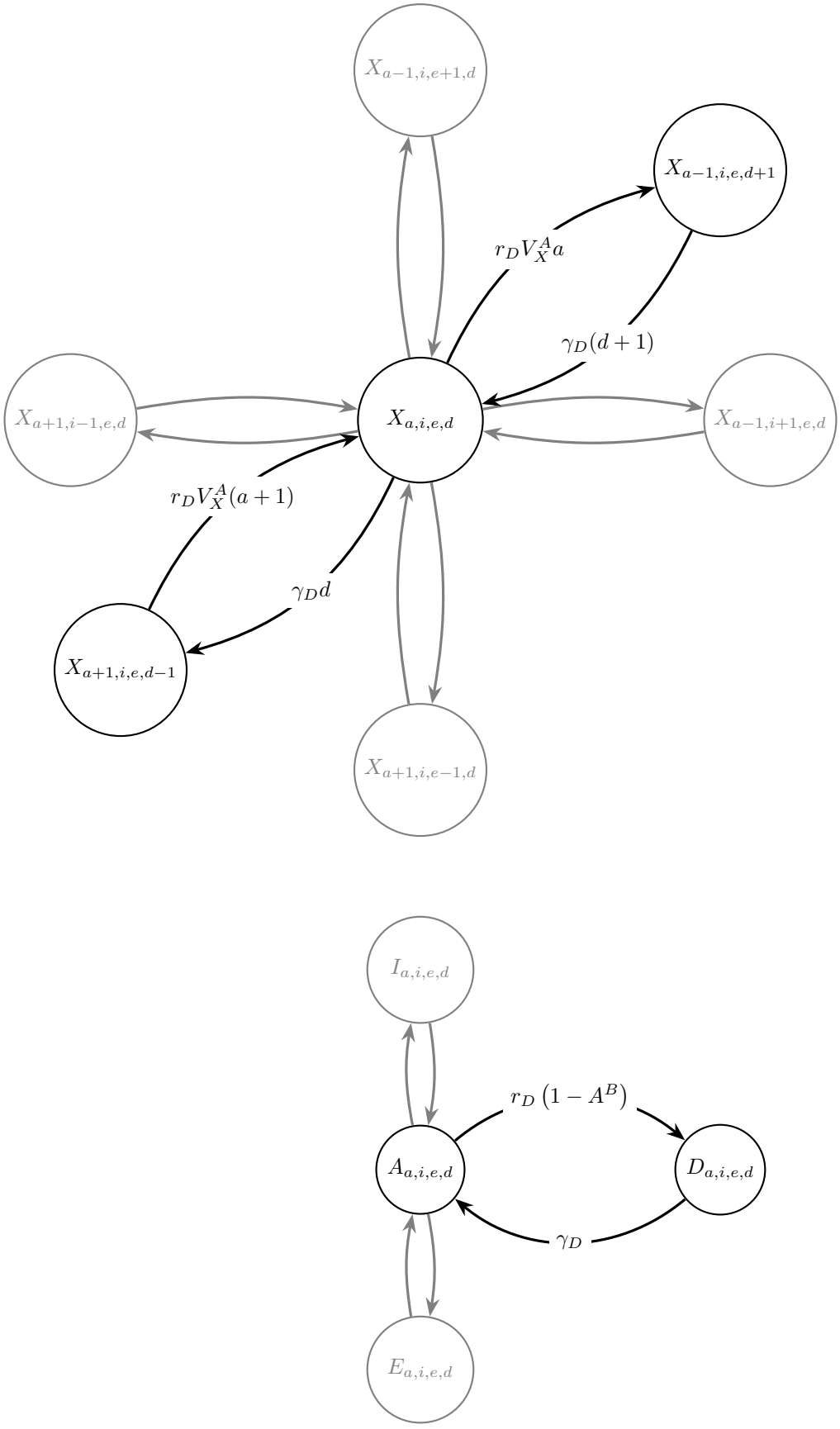

Figure 3.1: Top: Possible state transitions from center node $X(a,i,e)$ with transitions involving his neighbors. Bottom: Possible state transition of the center node itself. For the sake of readability we denote the state variable $X(a,i,e,d)$ by $X_{a,i,e,d}$. Also we only denote the rates of the transitions involved in dependency failure, the rates of the transitions indicated by gray arrows are as in figure 2.1.

$$\begin{aligned}\frac{d}{dt}I^A(a,i,e,d) =& p_A A^A(a,i,e,d) - \gamma_I I^A(a,i,e,d) \\ &+ p_A\big[(a+1)I^A(a+1,i-1,e,d) - aI^A(a,i,e,d)\big] \\ &+ \gamma_I\big[(i+1)I^A(a-1,i+1,e,d) - iI^A(a,i,e,d)\big] \\ &+ r_A W_A^A\big[(a+1)I^A(a+1,i,e-1,d) - aI^A(a,i,e,d)\big] \\ &+ \gamma_E\big[(e+1)I^A(a-1,i,e+1,d) - eI^A(a,i,e,d)\big] \\ &+ r_D V_X^A\big[(a+1)I^A(a+1,i,e,d-1) - aI^A(a,i,e,d)\big] \\ &+ \gamma_D\big[(d+1)I^A(a-1,i,e,d+1) - dI^A(a,i,e,d)\big]\end{aligned} \tag{3.4}$$

$$\begin{aligned}\frac{d}{dt}E^A(a,i,e,d) =& r_A\Theta(m-a)A^A(a,i,e,d) - \gamma_E E^A(a,i,e,d) \\ &+ p_A\big[(a+1)E^A(a+1,i-1,e,d) - aE^A(a,i,e,d)\big] \\ &+ \gamma_I\big[(i+1)E^A(a-1,i+1,e,d) - iE^A(a,i,e,d)\big] \\ &+ r_A W_A^A\big[(a+1)E^A(a+1,i,e-1,d) - aE^A(a,i,e,d)\big] \\ &+ \gamma_E\big[(e+1)E^A(a-1,i,e+1,d) - eE^A(a,i,e,d)\big] \\ &+ r_D V_X^A\big[(a+1)E^A(a+1,i,e,d-1) - aE^A(a,i,e,d)\big] \\ &+ \gamma_D\big[(d+1)E^A(a-1,i,e,d+1) - dE^A(a,i,e,d)\big]\end{aligned} \tag{3.5}$$

$$\begin{aligned}\frac{d}{dt}D^A(a,i,e,d) =& r_D(1-A^B) - \gamma_D D^A(a,i,e,d) \\ &+ p_A\big[(a+1)D^A(a+1,i-1,e,d) - aD^A(a,i,e,d)\big] \\ &+ \gamma_I\big[(i+1)D^A(a-1,i+1,e,d) - iD^A(a,i,e,d)\big] \\ &+ r_A W_A^A\big[(a+1)D^A(a+1,i,e-1,d) - aD^A(a,i,e,d)\big] \\ &+ \gamma_E\big[(e+1)D^A(a-1,i,e+1,d) - eD^A(a,i,e,d)\big] \\ &+ r_D V_X^A\big[(a+1)D^A(a+1,i,e,d-1) - aA^A(a,i,e,d)\big] \\ &+ \gamma_D\big[(d+1)D^A(a-1,i,e,d+1) - dA^A(a,i,e,d)\big]\end{aligned} \tag{3.6}$$

The evolution equations for network B are found by replacing the subscripts and superscripts A (B) of the state variables by B (A). We obtain a set of coupled equations, they form a closed system of deterministic equations.

3.2.2 Mean field equations

The mean field equations of the interconnected network are as in equation (3.7). For a derivation see appendix A.3.1.

$$\frac{dA^A}{dt} = \gamma_I I^A + \gamma_E E^A - p_A A^A - r_A \mathbf{s}(A^A) + \gamma_D D^A - r_D(1-A^B) \tag{3.7a}$$

$$\frac{dI^A}{dt} = p_A A^A - \gamma_I I^A \tag{3.7b}$$

$$\frac{dE^A}{dt} = r_A s(A^A) - \gamma_E E^A \tag{3.7c}$$

$$\frac{dD^A}{dt} = r_D^A(1-A^B) - \gamma_D D^A \tag{3.7d}$$

$$\frac{dA^B}{dt} = \gamma_I I^B + \gamma_E E^B - p_B A^B - r_B \mathbf{s}(A^B) + \gamma_D D^B - r_D(1-A^A) \tag{3.7e}$$

$$\frac{dI^B}{dt} = p_B A^B - \gamma_I I^B \tag{3.7f}$$

$$\frac{dE^B}{dt} = r_B s(A_B) - \gamma_E E^B \tag{3.7g}$$

$$\frac{dD^B}{dt} = r_D^B(1-A^A) - \gamma_D D^B \tag{3.7h}$$

In equation (3.7), for notational convenience, we used the following notation for the approximation of the fraction of active nodes within a network A.

$$\mathbf{s}(A) = A\sum_k f(k)\sum_{j=0}^{m}\binom{k}{j}(1-A)^{k-j}(A)^j \tag{3.8}$$

From equation (3.7) we obtain a set of two differential equations that are satisfied in the steady state as in equations (3.9a) and (3.9b), for a derivation see appendix A.3.1.

$$A^A = 1 - \frac{p_A}{\gamma_I}A^A - \frac{r_A}{\gamma_E}A^A\sum_k f(k)\sum_{j=0}^{m}\binom{m}{j}(1-A^A)^{k-j}(A^A)^j - \frac{r_D}{\gamma_D}(1-A^B) \tag{3.9a}$$

$$A^B = 1 - \frac{p_B}{\gamma_I}A^B - \frac{r_B}{\gamma_E}A^B\sum_k f(k)\sum_{j=0}^{m}\binom{m}{j}(1-A^B)^{k-j}(A^B)^j - \frac{r_D}{\gamma_D}(1-A^A) \tag{3.9b}$$

For fixed parameter values we can calculate fixed points of equations (3.9a) and (3.9b). Also we are able to determine their stability by linearization around the fixed points. For details on the linearization, please refer to appendix A.3.2.

The set of differential equations in equations (3.9a) and (3.9b) depends on the combination of parameter values

$$\frac{p_A}{\gamma_I}, \frac{p_B}{\gamma_I}, \frac{r_A}{\gamma_E}, \frac{r_B}{\gamma_E}, \frac{r_D}{\gamma_D}.$$

Therefore, in what follows we fix the recovery rates γ_I, γ_E and γ_D. Again, we use the more convenient parameter for internal failure p^* network A en B, as defined in equation (A.4), denoted by p_A^*, p_B^* respectively. Also, we assume that nodes in both networks fail externally at the same fixed rate, i.e. $r_A = r_B$. From this assumptions we predict symmetry in the phase diagram (p_A^*, p_B^*). Similar to [20], we set the rate at which nodes fail due to dependency failure $r_D = 0.1$.

3.2.3 Phase diagram

We continue with an investigation of the dynamics in the interconnected networks when varying the rate of internal failure for both networks by looking at the phase diagram (p_A^*, p_B^*). The system has four qualitatively different equilibria: LL, LH, HL and HH. Here the first and second letter corresponds to the state in the equilibrium of network A and B respectively, which can be low (L) active or high (H) active. Figures 3.2a to 3.2d show the existence of the stable equilibria LL, LH, HL and HH in the (p_A^*, p_B^*)-plane respectively. Additionally, figure 3.3 shows the phase diagram in which all four layers are combined. Note that the layers cover the total phase diagram, indicating that for all $p_A^*, p_B^* \in [0, 0.35]$ there exists at least one stable equilibrium. This indicates that for $r = 2$ the system does not exhibit oscillatory behavior.

In the following, we will illustrate the dynamics of both networks along the line $p_B^* = 0.22$. Note that this line crosses different regions of the phase diagrams in figure 3.3. This means the number of stable solutions as well as the behavior of both systems varies in p_A^*. Figure 3.4 shows the stable and unstable solutions of the system versus p_A^*.

Next, figures 3.5 to 3.9 show cross-sections of figure 3.4 for $p_A^* \in [0.05, 0.10, 0.15, 0.25, 0.30]$. For these five different values of p_A^* the system shows qualitatively different behavior. We investigate what happens when increasing p_A^*:

(i) For $p_A^* = 0.05$ we observe two stable solutions: HL and HH. Thus network A exhibits stable behavior, whereas network B exhibits bistable behavior.

(ii) For $p_A^* = 0.10$ we cross the blue line, indicating the appearance of equilibrium LL. Now, we observe three stable solutions: LL, HL and HH. Thus both networks exhibit bistable behavior.

(iii) For $p_A^* = 0.15$ we cross the red line, indicating the appearance of equilibrium LH. Now, we observe four stable solutions: LL, LH, HL and HH. Thus both networks exhibit bistable behavior.

(iv) For $p_A^* = 0.25$ we cross the yellow line and the red line, indicating the disappearance of equilibrium HL and LH respectively. Now, we observe two stable solutions: LL and HH. Still, both networks exhibit bistable behavior.

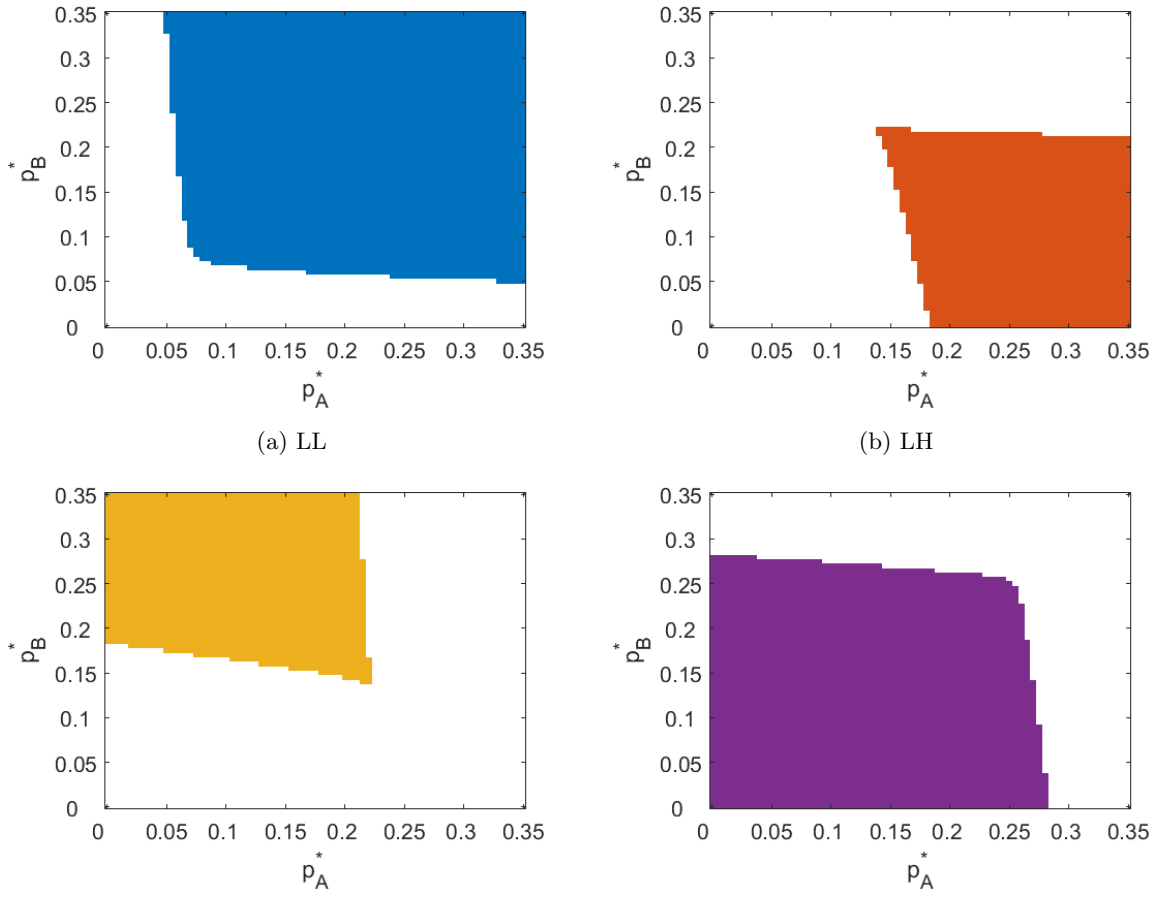

(a) LL (b) LH

(c) HL (d) HH

Figure 3.2: For two interconnected regular networks with $\bar{k} = 10, m = 4$ and parameter values $r_A = r_B = 2, \gamma_I = 0.01, \gamma_E = 1, \gamma_D = 1$. The phase diagrams show the regions where the stable equilibria (a) LL, (b) LH, (c) HL and (d) HH exist.

(v) For $p_A^* = 0.30$ we cross the purple line, indicating the disappearance of equilibrium HH. Now, we observe one stable solutions LL. So, both networks exhibit stable behavior.

We conclude that for $r_A = r_B = 2$ the phase diagram is very rich, we observed stable and bistable behavior for both networks. We have seen that only in the corners of the phase diagram in figure 3.3 both networks show stable behavior.

We continue with the phase diagram for $r_A = r_B = 1.5$. Figure 3.10 shows the existence of the four equilibria LL, LH, HL and HH. For this phase diagram the rate of external failure is smaller compared to the phase diagrams in figure 3.2, leading to higher activity of the networks. More specifically, the region where equilibrium HH exists becomes bigger, whereas the regions where equilibria LL, LH and HL exist become smaller. Furthermore, the phase diagram contains a region where none of the equilibria is stable, this may indicate the existence of an oscillatory region. We investigate this in section 3.2.3 by plotting stable and unstable solutions for $p_B^* = 0.15$ versus p_A^*. We indeed observe that for $p_A^* \in [0.31, 0.34]$ only one unstable solution is found in the closed system, thus the system exhibits oscillatory behavior.

In this chapter we introduced the failure-recovery model for interconnected networks. We used the effective degree approach to analytically study the system and we observed stable, bistable and oscillatory behavior of the system. In the rest of this thesis, we will only discuss single networks.

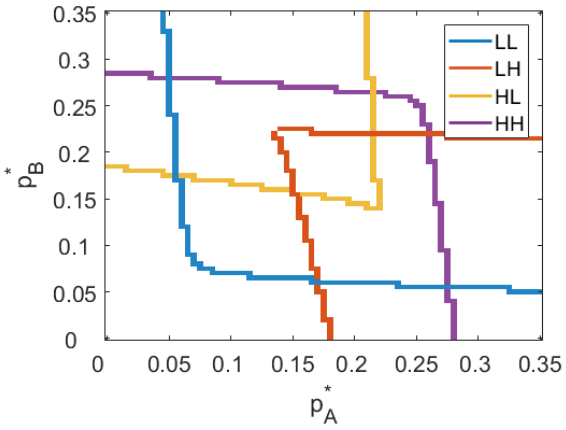

Figure 3.3: For two interconnected regular networks with $\bar{k} = 10, m = 4$ and parameter values $r_A = r_B = 2, \gamma_I = 0.01, \gamma_E = 1, \gamma_D = 1$. The phase diagram shows the borders of the regions where the stable equilibria LL, LH, HL and HH exist.

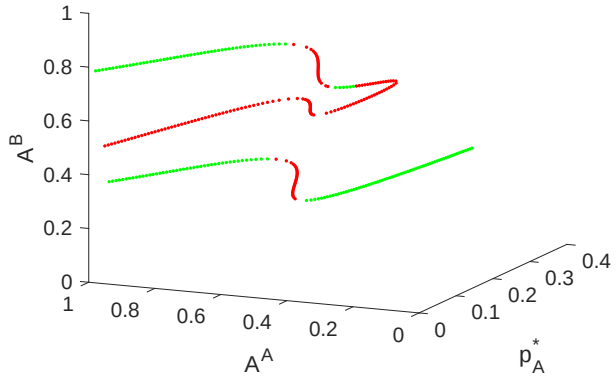

Figure 3.4: For two interconnected regular networks with $\bar{k} = 10, m = 4$ and parameter values $r_A = r_B = 2, r_D = 0.1, p_B^* = 0.22, \gamma_I = 0.01, \gamma_E = 1, \gamma_D = 1$. Stable (green dots) and unstable (red dots) solutions (A^A, A^B) versus p_A^*.

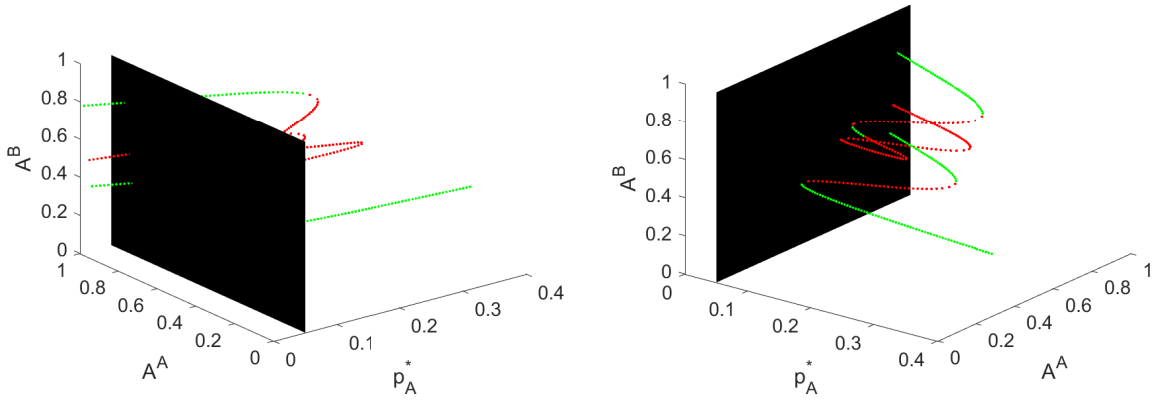

Figure 3.5: For two interconnected regular networks with $\bar{k} = 10, m = 4$ and parameter values $r_A = r_B = 2, r_D = 0.1, p_B^* = 0.22, \gamma_I = 0.01, \gamma_E = 1, \gamma_D = 1$. Stable (green dots) and unstable (red dots) solutions (A^A, A^B) versus p_A^* from two different angles, also shown is the cross-section for $p_A^* = 0.05$.

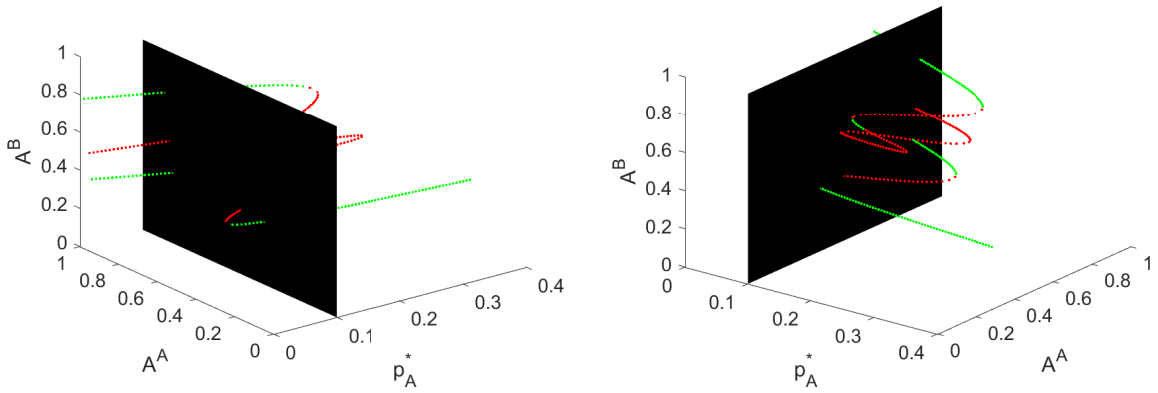

Figure 3.6: For two interconnected regular networks with $\bar{k} = 10, m = 4$ and parameter values $r_A = r_B = 2, r_D = 0.1, p_B^* = 0.22, \gamma_I = 0.01, \gamma_E = 1, \gamma_D = 1$. Stable (green dots) and unstable (red dots) solutions (A^A, A^B) versus p_A^* from two different angles, also shown is the cross-section for $p_A^* = 0.10$.

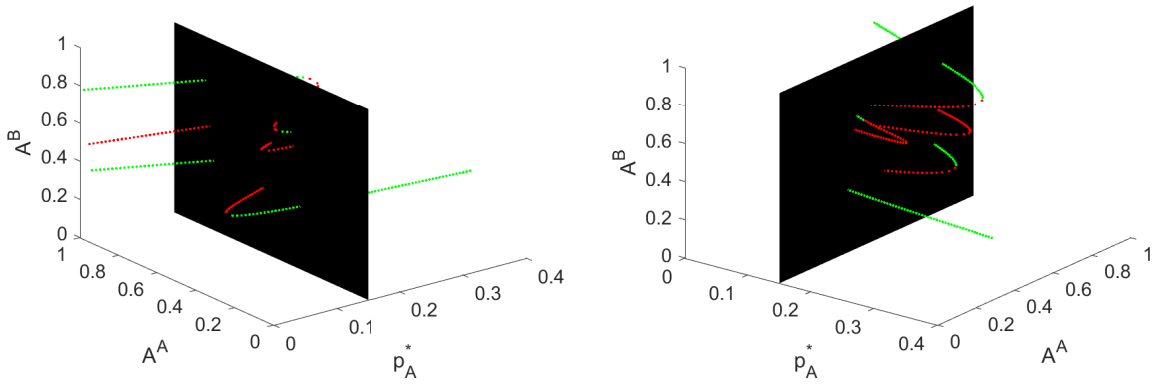

Figure 3.7: For two interconnected regular networks with $\bar{k} = 10, m = 4$ and parameter values $r_A = r_B = 2, r_D = 0.1, p_B^* = 0.22, \gamma_I = 0.01, \gamma_E = 1, \gamma_D = 1$. Stable (green dots) and unstable (red dots) solutions (A^A, A^B) versus p_A^* from two different angles, also shown is the cross-section for $p_A^* = 0.15$.

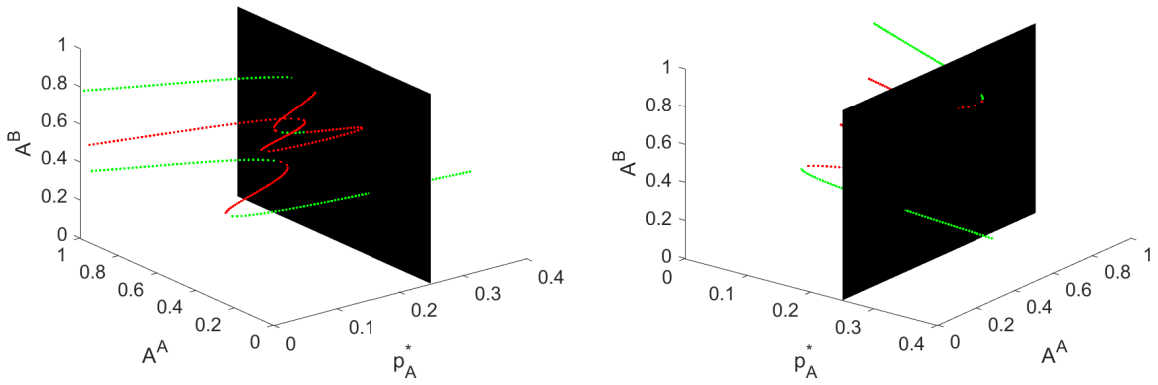

Figure 3.8: For two interconnected regular networks with $\bar{k} = 10, m = 4$ and parameter values $r_A = r_B = 2, r_D = 0.1, p_B^* = 0.22, \gamma_I = 0.01, \gamma_E = 1, \gamma_D = 1$. Stable (green dots) and unstable (red dots) solutions (A^A, A^B) versus p_A^* from two different angles, also shown is the cross-section for $p_A^* = 0.25$.

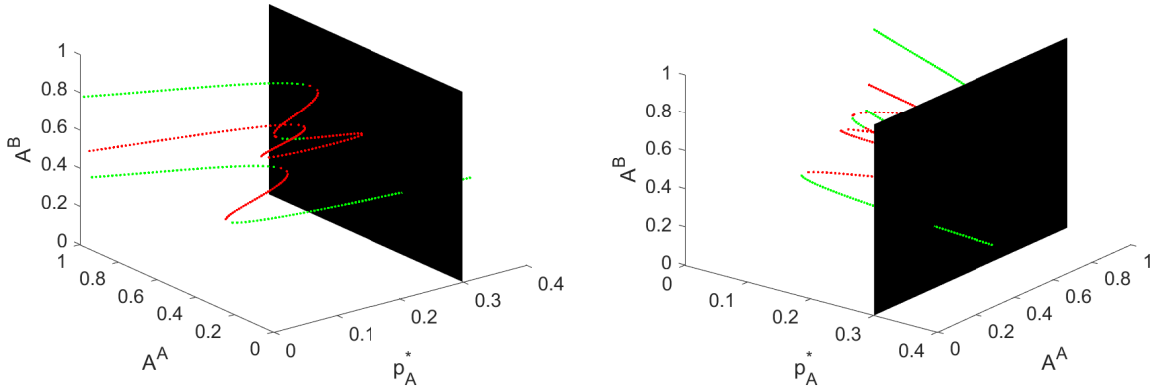

Figure 3.9: For two interconnected regular networks with $\bar{k} = 10, m = 4$ and parameter values $r_A = r_B = 2, r_D = 0.1, p_B^* = 0.22, \gamma_I = 0.01, \gamma_E = 1, \gamma_D = 1$. Stable (green dots) and unstable (red dots) solutions (A^A, A^B) versus p_A^* from two different angles, also shown is the cross-section for $p_A^* = 0.30$.

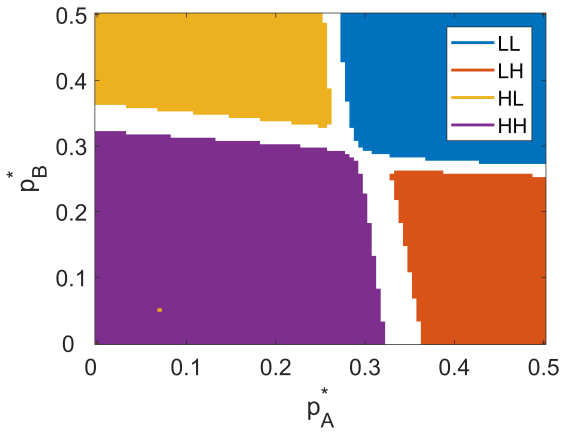

Figure 3.10: For two interconnected regular networks with $\bar{k} = 10, m = 4$ and parameter values $r_A = r_B = 1.5, r_D = 0.1, \gamma_I = 0.01, \gamma_E = 1, \gamma_D = 1$,. The phase diagram shows the regions where a different number of stable solutions are found.

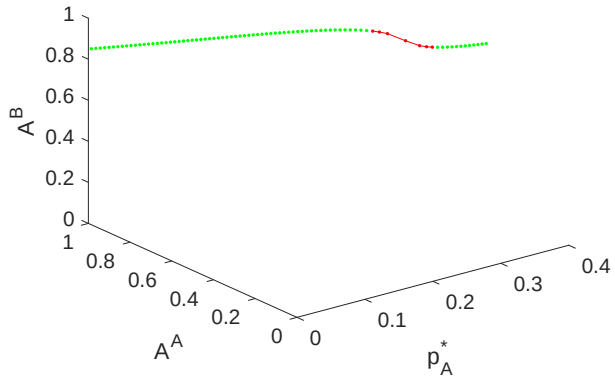

Figure 3.11: For two interconnected regular networks with $\bar{k} = 10, m = 4$ and parameter values $r_A = r_B = 1.5, r_D = 0.1, \gamma_I = 0.01, \gamma_E = 1, \gamma_D = 1$. A cross-section of the phase diagram for $p_B^* = 0.15$ shows the stable and unstable solutions (A^A, A^B) versus p_A^*. For $p_A^* \in [0.31, 0.34]$ only one unstable solution is found, indicating that the system exhibits oscillatory behavior.

Chapter 4

Exact stochastic simulation

In this chapter we aim to introduce exact stochastic simulation, which we will use in chapter 5 to study the dynamics in the failure-recovery model on non-regular networks. In these networks nodes are less homogeneous then nodes in a regular network; nodes differ by degree and may show clustering. To make the heterogeneity of nodes more suitable for detailed mathematical analysis, we will use the Gillespie algorithm presented in [10] to perform stochastic simulations.

In the remainder of this chapter, we will introduce the Gillespie algorithm. Additionally, we will discuss results of the stochastic simulations for regular networks to get familiar with the stochastic simulations. Not only will we discuss the influence of the size of the network and the number of stochastic realizations on the results, but we will also compare the stochastic results with the results obtained by the effective degree approach in chapter 2.

4.1 Gillespie algorithm

We consider the failure-recovery model as a Continuous Time Markov Chain with a discrete state space denoted by $X \in \mathbb{R}^N$, where N is the number of individuals in the network. In the model there are $i = 1, \ldots, v$ possible transition rates denoted by $h_i(X, c_i)$. Transition rate h_i depends only on the current state X and the rate constant c_i, i.e. p^*, r, γ_I and γ_E. Given the initial state of the system, the Gillespie algorithm decides the transition μ that takes place as well as the time interval $[t, t+\tau]$ in which it takes place.

The algorithm can be summarized as follows: [37, p.183]

1. Initialise the system at $t = 0$ with rate constants c_i for $i = 1, \ldots, v$ and initial condition of the state space X.
2. For each $i = 1, \ldots, v$ calculate $h_i(x, c_i)$ based on the current state X.
3. Calculate the sum of all possible transitions h_0, i.e.
$$h_0(X, c) = \sum_{i=1}^{v} h_i(X, c_i).$$
4. Draw a random number τ from the exponential distribution with mean $h_0(X, c)$, τ represents the time to the next event.
5. Update time, i.e. set $t = t + \tau$.
6. Draw a random number μ from the uniform distribution with probabilities $h_i(X, c_i)/h_0(X, c)$, for $i = 1, \ldots, v$. Here μ represents the transition that takes place during time interval $[t, t+\tau]$. So the probability that a transition takes place is proportional to its transition rate.
7. Update the state according to transition μ.
8. If $t < T_{max}$, return to step 2.

A discussion on the random numbers generation in step 4 and 6 of the algorithm is placed in appendix A.2.

4.2 Discussion

Real world networks are made up of a finite number of individuals. Strictly speaking, the notion of stability is only meaningful in the thermodynamic limit[3]. When the size of the system is to small, fluctuations can cause the system to switch between the two stable equilibria in the metastable domain. Therefore, the size of the system should be large to make fluctuation effects negligible. For example, in [26, 27, 32] stochastic simulations are performed for networks of size $N = 10^5$ and $N = 10^6$.

We will investigate the influence of the system size on the results of the stochastic simulations by using parameter values in the stable region, which we obtained with the effective degree approach in chapter 2. Results of the stochastic simulations for three different network sizes, i.e. $N = 10^5, N = 10^4$ and $N = 5 \times 10^3$, as well as results obtained by the effective degree approach for parameter values in the stable region are shown in figure 4.1.

Firstly, we observe that the fraction of active nodes obtained by the effective degree approach drops at a slightly different time compared to the simulation results due to stochastic effects[32]. Secondly, when increasing the size of the network, less stochastic fluctuations are present. Nevertheless, the system shows similar behavior and converges to the same equilibrium for different sizes of the network. Taking this into account, and also that simulations with networks of smaller sizes are more convenient due to computational limitations, in chapter 5 we will use networks of size $N = 5 \times 10^3$.

To get a statistically complete picture of the temporal evolution of the system, [10] reports that we must carry out several independent realizations of the Gillespie algorithm, each starting with the same initial state and proceeding to the same time T. In practice, somewhere between 3 and 10 runs should provide a statistically adequate picture of the state of the system at time T[10].

Next, we will investigate the influence of the number of realizations of the stochastic simulation on the results by performing three independent stochastic simulations for a regular network of size $N = 5 \times 10^3$. To do this, we use two different combinations of parameter values for which the system shows stable and oscillatory behavior, respectively shown in figure 4.2a and figure 4.2b. Additionally, both figures show the results obtained by the effective degree approach. As observed above, due to stochastic effects, the sudden drop in the fraction of active nodes in the stochastic realizations occurs at a different time compared to the results obtained by the effective degree approach. Nevertheless, the stochastic simulations show oscillations of (approximately) the same period. We observe that the three realizations are in good agreement, indicating that only a small number of runs is enough to draw results.

To summarize, in this chapter we have seen that stochastic simulations with the Gillespie algorithm give an accurate picture of the evolution of the system. We also observed that we obtained accurate results for a small number of realizations for networks of size $N = 5 \times 10^3$.

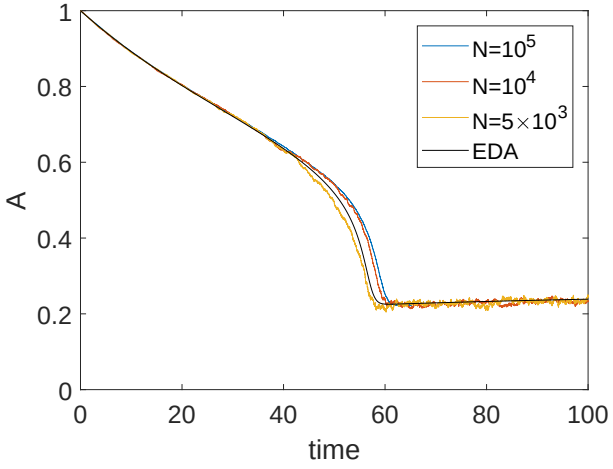

Figure 4.1: The time evolution of active nodes for a regular network with $\bar{k} = 10, m = 4$ and parameter values $p^* = 0.7, r = 2, \gamma_I = 0.01, \gamma_E = 1$. The stochastic simulation results for networks of size $N = 10^5, N = 10^4$ and $N = 5 \times 10^3$ and results obtained by the effective degree approach are shown.

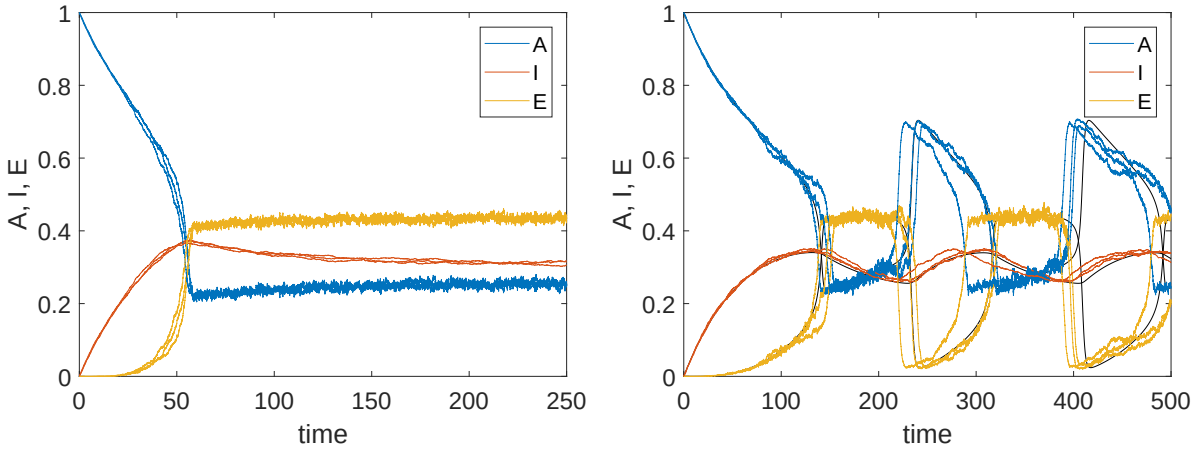

(a) (b)

Figure 4.2: The time evolution of active, internally failed and externally failed nodes for a regular network of size $N = 5 \times 10^3, \bar{k} = 10$ and $m = 4$ and parameter values $\gamma_I = 0.01$ and $\gamma_E = 1$. Results from the effective degree approach (black) as well as the results of three stochastic simulations are shown. (a) For parameter values $(r, p^*) = (2, 0.7)$, the system shows stable behavior. (b) For parameter values $(r, p^*) = (2, 0.5)$, the system shows oscillatory behavior.

Chapter 5

Robustness

The topology of the network has a great influence in the overall dynamic behavior of the system; therefore, in this chapter we will consider four networks with different properties. We aim to investigate the robustness of the different network types by performing stochastic simulations.

Generally speaking, a network is robust if its nodes are able to function even when a large fraction of its nodes have failed[26]. In models without recovery, the resilience of a complex network is often characterized by the integral size of the giant component during the whole attacking process or defined by the percolation thresholds[4, 9, 29]. As in [26], our definition of robustness is dynamic, i.e., the more robust a network is, the longer it will last. In other words, for some fixed parameters of internal and external failure we say that the robustness is enhanced when the system stays longer in a high-active phase. As in the percolation models we use the percolation threshold to compare the robustness of different networks. In the simplest case the parameter space is one-dimensional. Then the percolation threshold is the critical value of the parameter for which the system undergoes a first order phase transition. Since our parameter space (r, p^*) is two-dimensional, we will fix r to obtain the critical threshold p_c^*.

This chapter is organized as follows. First, we will introduce four different network types which we distinguish by their local properties. Subsequently, we will investigate the robustness of these networks.

5.1 Networks

In this section we will introduce four different network types. To be able to distinguish between these types we will look at their clustering coefficients, characteristic path lengths and degree distribution. We will look at these terms first, and then introduce the networks with these terms in mind.

We measure the clustering coefficient and the characteristic path length by definitions 1 and 2 respectively[28].

Definition 1 (Clustering coefficient)**.** *For a network of size N, we define $E^i \in \mathbb{R}^{N\times N}$ as the adjacency matrix of the neighbors of node i. So, $E^i_{j,k} = 1$ if node j and node k are both neighbors of node i and node j and k are connected. The clustering coefficient of node i is a measure of its local connectedness. For a node i the clustering is defined as the number of links between neighbors divided by the possible number of such links $\frac{k_i(k_i-1)}{2}$, i.e. the following.*

$$C_i = \frac{|E^i|}{\frac{k_i(k_i-1)}{2}}$$

With that in mind, the network average clustering coefficient equals the following.

$$\bar{C} = \frac{1}{N}\sum_{i=1}^{N} C_i$$

Definition 2 (Characteristic path length)**.** *Consider an adjacency matrix A which represents the connections between N nodes. Let $d(i, j)$ be the shortest distance between i and j. Assume that $d(i, j) < \infty$ for all i, j, i.e. assume that the network is connected. Then the characteristic path length, which is just*

the average shortest path length between all nodes in the network, is defined by the following.

$$l = \frac{1}{N(N-1)} \sum_{i \neq j} d(i,j)$$

Two common classes of networks are homogeneous networks with a Poisson degree distribution and heterogeneous networks with a power-law degree distribution[29]. These networks have a narrow degree distribution and a broad degree distribution respectively.

Many real systems are dynamically evolving (i.e., edges are added or rewired) with time, or influenced by other factors[9]. Think of technological networks, where backup channels and rerouting protocols are accessible. On the other hand, in infrastructure networks the creation of new physical links is constrained, and the systems are static rather than dynamic. In this thesis, we will focus on static networks. We continue with a brief introduction of the four network types: we will mention their main properties and we will explain how they can be constructed.

The first type of network that we consider are the regular networks, which we have already used in chapter 2. Here all nodes are of degree k, and the network can be constructed by the configuration model[22]. The model starts from N nodes, each node has k half edges. The $N \cdot k$ half edges are paired and glued together at random, creating a network with all nodes of equal degree k, resulting in a narrow degree distribution. Regular networks have short characteristic path length and low clustering.

The second type of network that we consider are the Erdös-Rényi networks, which fall in the class of Random networks. An Erdös-Rényi network with average degree k is constructed by placing an edge between two nodes with probability k/N. This means that the probability of a node having degree k is given by the following, where z is equal to the mean degree k/N(N-1)[22].

$$p_k = \binom{n}{k} p^k (1-p)^{n-k} \approx \frac{z^k e^{-z}}{k!}$$

From this, we conclude the degree distribution of an Erdös-Rényi network is Poisson. Also, from definitions 1 and 2 follows that the network has short characteristic path lengths and does not show clustering.

Real world complex networks are known to have short characteristic path lengths and high clustering[16]. The short characteristic path length is found in Erdös-Rényi networks, but these networks do not show clustering. Opposite to the Erdös-Rényi networks are the regular ring networks, where nodes are placed in a ring and all nodes are connected to their k closest neighbors. These networks show long characteristic path lengths and high clustering. To mimic real world networks, we seek a network that exhibits the short characteristic path length of the Erdös-Rényi network and the high clustering of the regular ring network.

The third type of network we consider are the Watts-Strogatz networks. We use the Watts-Strogatz model to tune between Erdös-Rényi networks and regular ring networks. The model starts from a regular ring network, and rewires the endpoint of each link to a random link with a probability β. Here the parameter β controls the randomness of the network: for $\beta = 0$ we have a ring lattice, and for $\beta = 1$ we have an Erdös-Rényi network.

In figure 5.1 the characteristic path length and the clustering coefficient are plotted versus rewiring parameter β. We want to find the value of β such that we obtain networks with short paths between nodes, but nodes also show high clustering. In what follows, we set the rewiring parameter $\beta = 10^{-2}$, because for this value the network shows a small characteristic path length (12.2976) and a high clustering coefficient (0.6474). In what follows, if we do not mention the value of β, it is set equal to 10^{-2}. For this value of β, the Watts-Strogatz model results in a network with a narrow degree distribution.

An inconsistency in the three networks we discussed so far, is that none of them reproduce networks with hubs (i.e. a small number of nodes with a much larger than average number of edges to/from other nodes). This property is also known as scale-free[28]. Networks that can be approximated as scale-free networks include the World Wide Web, social networks, infrastructure networks, networks in biology, and networks in physics[8].

The fourth type of network that we consider are the Barabási and Albert networks, which are based on a preferential attachment mechanism and produce a network with a power law degree distribution[2]. The Barabási model starts from a network with a small number of nodes, and in every step a node is added to the network. The new node is connected to the existing nodes with a probability proportional to the degree of the nodes. We note that the Barabási and Albert model mimics a natural process of two interdependent growing networks. For example, in terms of a power network and a communication

network, newly developed areas are populated and connected to infrastructures at different times[24]. In what follows, we will refer to this type of networks as Barabási networks. The Barabási network shows a short characteristic path length. A disadvantage of this type of network is that it does not reproduce the small-world property, since it shows low clustering[28].

Table 5.1 summarizes the characteristic path length, clustering coefficient and broadness for all networks. The homogeneous degree distribution of the Erdös-Rényi and Watts-Strogatz network is shown in figure 5.2a. We observe that the degree distribution of the Watts-Strogatz network is narrower than the degree distribution of the Erdös-Rényi network, something we will also discuss in section 5.2. Additionally, figure 5.2b shows the heterogeneous degree distribution of the Barabási network.

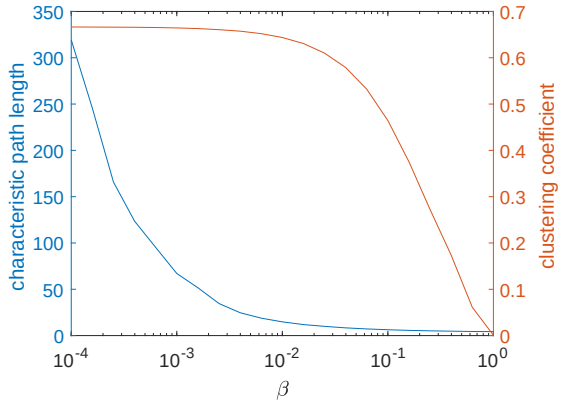

Figure 5.1: For networks of size $N = 5 \times 10^3$ and $\bar{k} = 10$. The rewiring parameter β versus the characteristic path length and clustering coefficient. The model of Watts and Strogatz starts from a regular ring lattice for $\beta = 0$ and for $\beta = 1$ it is evolved to an Erdös-Rényi network. Note that we used logarithmic scaling on the horizontal axis.

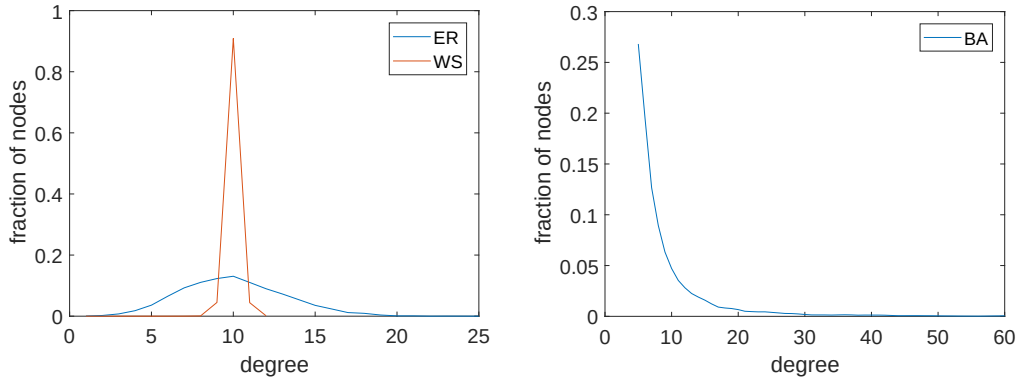

(a) (b)

Figure 5.2: For networks of size $N = 5 \times 10^3$ and $\bar{k} = 10$. (a) The narrow degree distribution of the Erdös-Rényi network and the Watts-Strogatz network. (b) The broad degree distribution of the Barabási network.

Network	regular	Erdös-Rényi	Watts-Strogatz	Barabási
Characteristic path length	4.0039	3.9481	12.2976	3.4664
Clustering coefficient	0.0016	0.0020	0.6474	0.0182
Degree distribution	narrow	narrow	narrow	broad

Table 5.1: Characteristic path length, clustering coefficient and degree distribution for each of the four types of networks. For networks of size $N = 5 \times 10^3$ and $\bar{k} = 10$. Results are averaged over 50 network realizations. The Watts-Strogatz networks are constructed for $\beta = 10^{-2}$.

5.2 Method and Results

In this section we will investigate the robustness of the four different types of networks. First, we will look at the method used, and then we will move on to the results.

To compare the robustness of the different network types, we performed stochastic simulations with the Gillespie algorithm. For every network type (i.e. regular, Erdös-Rényi, Watts-Strogatz, Barabási) and for every $r \in \{1, 2, 3, 4\}$ we calculate the stable solutions versus $p^* \in [0, 1]$ as follows. For every value of p^* we run the Gillespie algorithm for 300 time units and if the system stabilizes we calculate the stable solution by averaging over the last 100 time units.

The stable solutions of A versus p^* for all network types are shown in figures 5.3a to 5.3d for $r = \{1, 2, 3, 4\}$ respectively. In the following, we will make some observations on the behavior of all networks.

We observe that the Barabási network shows, compared to the other networks, lower activity for $p^* < 0.4$. We speculate that this is due to its broad degree distribution. This can be intuitively be understood as follows. The probability for a node to have a damaged neighborhood depends on its degree: the higher the degree of a node, the less vulnerable it is to external failure. Therefore, for small p^*, we expect that the externally failed nodes are predominantly low degree nodes. We can verify this argument by looking at the average degree of active nodes.

In figures 5.4a and 5.4b we show the fraction of active, internally failed and externally failed nodes versus p^*, and the average degree of the active nodes versus p^* respectively. We observe that the average degree of the active nodes is above 10, which is the average degree of the total network. Additionally, we observe that the average degree of the active nodes and the fraction of externally failed nodes are increasing on the same domain. From this we conclude that the broad distribution of the Barabási network explains the high external failure for small p^*.

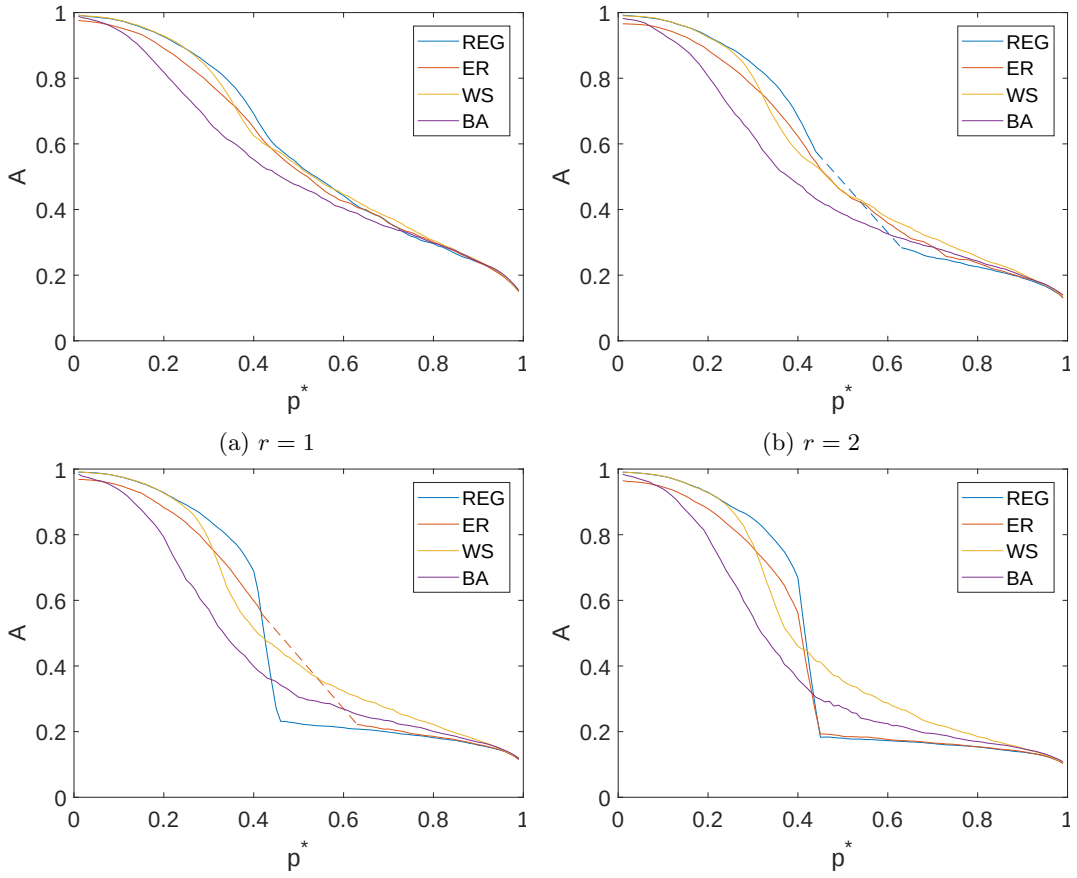

(a) $r = 1$ (b) $r = 2$

(c) $r = 3$ (d) $r = 4$

Figure 5.3: For the regular, Erdös-Rényi, Watts-Strogatz and Barabási networks of size $N = 5 \times 10^3$, with $\bar{k} = 10, m = 4$ and parameter values $\gamma_I = 0.01, \gamma_E = 1$. The stable fraction of active nodes A versus p^* for different values of r. The oscillatory regions are indicated by a dashed line.

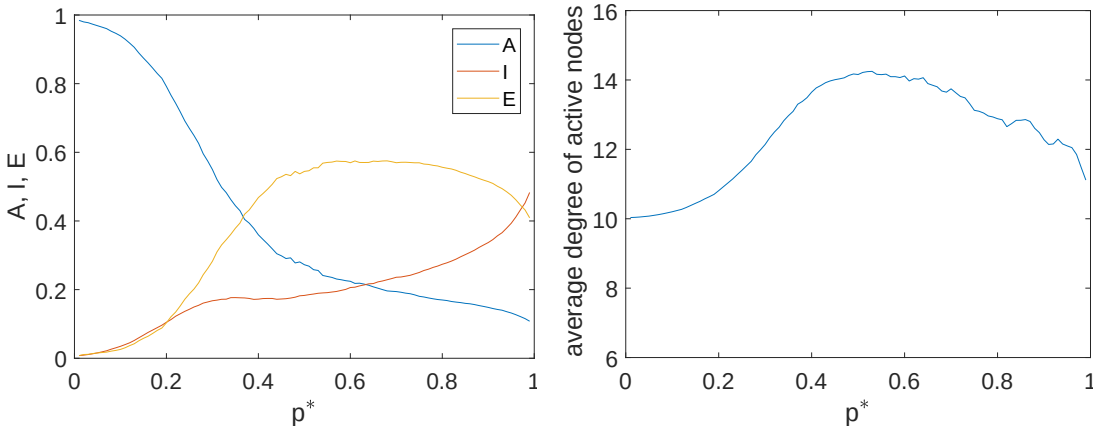

(a) (b)

Figure 5.4: For the Barabási network of size $N = 5 \times 10^3$, with $\bar{k} = 10, m = 4$ and parameter values $r = 4, \gamma_I = 0.01, \gamma_E = 1$. (a) The fraction of active nodes, internally failed nodes and externally failed nodes versus p^*. (b) The average degree of the active nodes versus p^*.

Next, in figure 5.3 we observe that transitions become sharper for all network types when we increase the rate of external failure r. This can be explained by the fact that by increasing r, external failure becomes more prevalent than both recovery and internal failure. Therefore, the system switches to a low active state more quickly, which makes the transition sharper.

For high rates of external failure, we observe that the regular and Erdös-Rényi networks show a first order phase transition, meaning that there is a discontinuity in the first derivative of A. This can be understood intuitively by the following reasoning. The degree distributions of both networks are very homogeneous; therefore, when the fraction of active nodes is below some threshold value, a predominant part of the network has a damaged neighborhood. As the rate of external failure is high, this predominant part of the nodes will fail externally in a small time interval. This leads to a first order phase transition.

Note that in the regular network all nodes have the same degree. This makes the time interval in which the predominant part of the nodes fail externally even shorter. This explains why the transitions of the regular network are sharper than the transitions in the Erdös-Rényi network, where nodes do not all have the same degree.

Another common feature of the regular network and the Erdös-Rényi network is that they both show oscillatory behavior. The oscillatory behavior for the regular network and the Erdös-Rényi network for $r = 2$ and $r = 3$ respectively, is indicated by a dashed line in figure 5.3. As nodes are homogeneous, competition between internal and external failure is present. This is what we have also seen in chapter 2.

We continue with the Watts-Strogatz network. In figure 5.2a we have seen that the degree distribution of this network is very narrow. As the degree distribution of the Watts-Strogatz network is more narrow than the degree distribution of the Erdös-Rényi network, we could expect oscillatory behavior in figure 5.3, as well as a first order phase transition in A. We do not observe oscillatory behavior for the Watts-Strogatz network. However, we have seen that the range in which we find oscillatory behavior for the regular and the Erdös-Rényi network is very small. Therefore, it is also possible that the Watts-Strogatz network does exhibit oscillatory behavior, but that we do not detect it. We also do not observe a first order transition, but instead see smooth behavior of the stable solutions for the Watts-Strogatz network. This observation contradicts the previous argument where we said that networks with a homogeneous distribution show a first order phase transition.

A difference between the Watts-Strogatz network and the Erdös-Rényi/regular network is found in the path length and the clustering. We speculate that these two parameters influence robustness. Therefore, in what follows, we aim to find the influence of path length and clustering on robustness. In section 5.1 we discussed the construction of the Watts-Strogatz network and decided to set the rewiring parameter at $\beta = 10^{-2}$, because for this value the network shows low characteristic path length and high clustering. We can vary the path length and the clustering by setting the rewiring parameter to different values of β to investigate their influence on the robustness. Table 5.2 shows the characteristic path length and clustering coefficient for five different values of (rewiring parameter) β. Additionally, figure 4.5 shows the degree distribution for different values of β. We observe that the degree distribution becomes broader

	$\beta = 0$	$\beta = 10^{-3}$	$\beta = 10^{-2}$	$\beta = 10^{-1}$	$\beta = 10^{-0.6}$	$\beta = 1$
Characteristic path length	250.45	48.65	12.30	5.62	4.61	3.97
Clustering coefficient	0.67	0.66	0.65	0.49	0.28	0.00

Table 5.2: For the Watts-Strogatz network of size $N = 5 \times 10^3$ and average degree $\bar{k} = 10$. The characteristic path length and the clustering for different values of rewiring parameter β. Results are averaged over 50 network realizations and tabulated to two decimals.

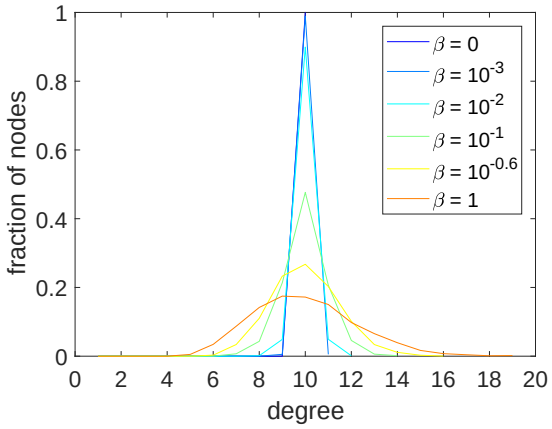

Figure 5.5: For networks of size $N = 5 \times 10^3$ and $\bar{k} = 10$. Plot of the degree distribution for the Watts-Strogatz network for different values of β. The distribution becomes broader when increasing β. Note that for $\beta = 1$ the Watts-Strogatz network is equal to the Erdös-Rényi network.

when increasing β.

First, we consider three different Watts-Strogatz networks for $\beta = 0$, $\beta = 10^{-3}$ and $\beta = 10^{-2}$. In table 5.2 we observe that for these values of β the clustering is constant, but the path length decreases with β. The stable solutions of A are plotted versus p^* in figure 5.6 for the three values of β. We observe that the behavior of the system does not differ as β changes. From this we conclude that path length does not influence the robustness of the Watts-Strogatz network.

Second, we consider the Watts-Strogatz network for $\beta = 0$, $\beta = 10^{-1}$, $\beta = 10^{-0.6}$ and $\beta = 1$. In table 5.2 we observe that the clustering decreases in β. Recall that the Watts-Strogatz network for $\beta = 0$ is a regular ring lattice and for $\beta = 1$ all edges are rewired, resulting in an Erdös-Rényi network. The stable solutions of A are plotted versus p^* in figure 5.6. Note that for $\beta = 10^{-0.6}$ the system exhibits oscillatory behavior for $p^* \in [0.38, 0.52]$. Also, we observe that the behavior of the system is smoother for smaller β, so increasing the clustering in the Watts-Strogatz network makes the behavior smoother. From this we conclude that clustering in the Watts-Strogatz network explains its smooth behavior. More specifically, increasing clustering in the Watts-Strogatz network makes the system less robust: the system stays in the high-active phase shorter.

We end this chapter by summarizing the main results. First, we conclude that the heterogeneous degree distribution of the Barabási network makes low-degree nodes very vulnerable against failure, whereas the hubs are very robust against failure. Therefore, initially the Barabási network shows high failure compared to the other networks.

Secondly, we conclude that unclustered networks with a homogeneous degree distribution, such as the regular and Erdös-Rényi network, are initially higher active than clustered networks and networks with a heterogeneous degree distribution. But, for high r, these networks eventually show a first order phase transition, which makes the nodes in the networks less active compared to the other networks.

Thirdly, we conclude that increasing clustering in the Watts-Strogatz network makes the network less robust. Even though the Watts-Strogatz network has a narrow degree distribution we do not observe a first order phase transition. The smooth behavior of the Watts-Strogatz network is explained by its local characteristics. We have seen that characteristic path length does not influence the robustness of the network, whereas increasing clustering makes the network less robust. Also, we conclude that a first order phase transition is only observed for networks with a homogeneous degree distribution where the nodes do not show clustering.

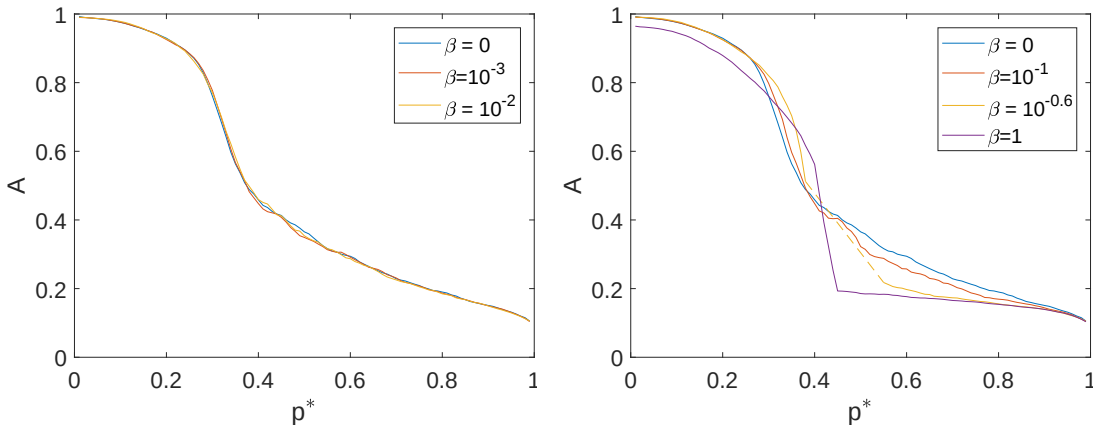

(a) (b)

Figure 5.6: For networks of size $N = 5 \times 10^3$, with $\bar{k} = 10$, $m = 4$ and parameter values $r = 4, \gamma_I = 0.01, \gamma_E = 1$. The stable solutions of A versus p^* for Watts-Strogatz networks for different values of β. (a) For values of β with (approximately) constant clustering coefficient, whereas the characteristic path length is decreasing in β. (b) For different values of β, the clustering coefficient is decreasing in β.

Chapter 6

Conclusion

In this thesis we discussed the failure-recovery model for single networks in which nodes can fail due to internal failure and external failure, and in which nodes may recover from failure. This model mimics the spread of stress on the work floor. We aimed to investigate the robustness of different networks.

First, in chapter 2 we used the effective degree approach to analytically study the model. We derived ODEs and mean field equations to describe the behavior of the system. We divided the phase diagram into a stable region, a bistable region and an oscillatory region. Also, we briefly discussed the possibility for external failed nodes to fail internally. We have seen that by including this extra transition, the oscillatory behavior of the system vanishes.

In chapter 3 we introduced the failure-recovery model for interconnected networks. In this model we introduced the dependency failure. We again used the effective degree approach to analytically treat the model in the case of two interconnected regular networks. We illustrated the behavior of the system and obtained a rich phase diagram.

In chapter 4 we introduced stochastic simulation to study networks in which the nodes are more heterogeneous compared to the nodes in a regular network. Subsequently, in chapter 5, we discussed four network types: regular, Erdös-Rényi, Watts-Strogatz and Barabási networks. We distinguished these networks by their local properties of clustering and path length. Next we investigated their robustness, we continue by summing up the main results and giving some recommendations on network structures in the context of the workplace.

We concluded that homogeneous, unclustered networks, such as the regular and the Erdös-Rényi network, are very robust against failure. However, these networks also showed a critical transition in which the density of active nodes drops sharply. Also, we observed oscillatory behavior in these networks for some small range of parameter values. The observed critical transition as well as the oscillatory behavior makes the behavior on these networks unpredictable.

Furthermore, we considered the Watts-Strogatz network, which showed short characteristic path length and high clustering. We concluded that the robustness is not influenced by the characteristic path length. We also concluded that increasing the clustering in the Watts-Strogatz network makes the network less robust.

Lastly, we concluded that the Barabási network, the network with broad degree distribution, is very vulnerable to failure. Assuming that all nodes need the same number of active neighbors to be not vulnerable to external failure makes hubs very robust against failure, whereas the nodes of low degree are very vulnerable.

Based on these findings we make some recommendations to limit the spread of stress in the workplace. First, under the assumptions of our model the results for the Barabási network showed that including some nodes of high-degree in the network may improve the robustness. Secondly, it is recommended to avoid clustering in the network, we have seen for the Watts-Strogatz network that increasing the clustering decreases the robustness. Thirdly, we observed that path length does not influence the robustness of the network, therefore this is something that should not be taken into account when considering the network structure of an organization. Fourthly, unclustered networks in which the nodes are homogeneous may show unpredictable behavior similar to the Erdös-Rényi and regular networks.

Limitations and further research

We continue with a discussion on the limitations of this research and give some suggestions for further research.

The presented derivation in chapters 2 and 3 only considers an analytic treatment for regular networks- other network structures are not analytically studied. Also, for the interconnected networks only a one-to-one random coupling is studied.

Furthermore, the robustness of different networks is only studied for the single network and not for the interconnected network. It may be interesting to also use stochastic simulations to study the robustness of interconnected networks. Not only the role of the coupling of different types of networks on the robustness can be studied, but also the role of the type of coupling can be clarified in further studies.

Under the assumptions of this thesis, nodes of high degree in the Barabási networks are very robust against failure. In the context of the spread of stress in the workplace this mimics a situation where individuals with a lot of connections within the network rarely experience external failure. This assumption is not substantiated by literature, and needs further investigation. To discard this assumption, a fractional threshold for the number of active neighbors may be considered instead of an absolute one.

An unrealistic feature of the model is that all nodes behave homogeneously; failure happens under the same assumptions for all nodes. It would be interesting to study networks in which some nodes behave differently. Think for example of nodes that do not recover, which mimics the situation in the workplace where individuals become incapacitated. Another option is to consider nodes that only fail externally and not internally, which represents the individuals that are only influenced by their colleagues.

In further studies, the interpretation of the mapping from a mathematical network to a network in an organization should be discussed. First, the interpretation of links between individuals should be specified; do the links between individuals only represent formal contacts or also social contacts? Secondly, assume that the failure-recovery model finds an optimal network structure to prevent the spread of stress. To what extent can this network structure be imitated within the organization? For example, how are links between individuals created and removed, and will this optimal network structure lead to a workable setting?

Bibliography

[1] Allen, L. J., Brauer, F., Van den Driessche, P., & Wu, J. (2008). *Mathematical epidemiology (1st ed.)*. Berlin: Springer.

[2] Barabási, A. L., & Albert, R. (1999). Emergence of scaling in random networks. *Science, 286*(5439), 509-512.

[3] Böttcher, L., Luković, M., Nagler, J., Havlin, S., & Herrmann, H. J. (2017). Failure and recovery in dynamical networks. *Scientific Reports, 7*, 41729.

[4] Buldyrev, S. V., Parshani, R., Paul, G., Stanley, H. E., & Havlin, S. (2010). Catastrophic cascade of failures in interdependent networks. *Nature, 464*(7291), 1025-1028.

[5] Buldyrev, S. V., Shere, N. W., & Cwilich, G. A. (2011). Interdependent networks with identical degrees of mutually dependent nodes. *Physical Review E, 83*(1), 016112.

[6] Cho, W. K., Goh, K. I., & Kim, I. M. (2010). Correlated couplings and robustness of coupled networks. Retrieved from https://arxiv.org/abs/1010.4971

[7] Gao, J., Buldyrev, S. V., Havlin, S., & Stanley, H. E. (2011). Robustness of a network of networks. *Physical Review Letters, 107*(19), 195701.

[8] Gao, J., Buldyrev, S. V., Stanley, H. E., & Havlin, S. (2012). Networks formed from interdependent networks. *Nature Physics, 8*(1), 40-48.

[9] Gao, J., Liu, X., Li, D., & Havlin, S. (2015). Recent progress on the resilience of complex networks. *Energies, 8*(10), 12187-12210.

[10] Gillespie, D. T. (1976). A general method for numerically simulating the stochastic time evolution of coupled chemical reactions. *Journal of Computational Physics, 22*(4), 403-434.

[11] Gleeson, J. P. (2013). Binary-state dynamics on complex networks: Pair approximation and beyond. *Physical Review X, 3*(2), 021004.

[12] Gong, M., Ma, L., Cai, Q., & Jiao, L. (2015). Enhancing robustness of coupled networks under targeted recoveries. *Scientific Reports, 5*.

[13] Gu, C. G., Zou, S. R., Xu, X. L., Qu, Y. Q., Jiang, Y. M., Liu, H. K., & Zhou, T. (2011). Onset of cooperation between layered networks. *Physical Review E, 84*(2), 026101.

[14] Hong, S., Lv, C., Zhao, T., Wang, B., Wang, J., & Zhu, J. (2016). Cascading failure analysis and restoration strategy in an interdependent network. *Journal of Physics A: Mathematical and Theoretical, 49*(19), 195101.

[15] Kiss, I. Z., Miller, J. C., & Simon, P. L. (2017). *Mathematics of Epidemics on Networks*. Berlin: Springer.

[16] Lang, J., De Sterck, H., Kaiser, J. L., & Miller, J. C. (2017). Random Spatial Networks: Small Worlds without Clustering, Traveling Waves, and Hop-and-Spread Disease Dynamics. Retrieved from https://arxiv.org/abs/1702.01252v1.

[17] Lindquist, J., Ma, J., Van den Driessche, P., & Willeboordse, F. H. (2011). Effective degree network disease models. *Journal of Mathematical Biology, 62*(2), 143-164.

[18] Liu, C., Li, D., Zio, E., & Kang, R. (2014). A modeling framework for system restoration from cascading failures. *PloS ONE, 9*(12), e112363.

[19] Majdandzic, A. (2016). Recovery processes and dynamics in single and interdependent networks (Doctoral dissertation, Boston University).

[20] Majdandzic, A., Braunstein, L. A., Curme, C., Vodenska, I., Levy-Carciente, S., Stanley, H. E., & Havlin, S. (2016). Multiple tipping points and optimal repairing in interacting networks. *Nature Communications, 7*.

[21] Majdandzic, A., Podobnik, B., Buldyrev, S. V., Kenett, D. Y., Havlin, S., & Stanley, H. E. (2014). Spontaneous recovery in dynamical networks. *Nature Physics, 10*(1), 34.

[22] Newman, M. E. (2003). The structure and function of complex networks. *SIAM Review, 45*(2), 167-256.

[23] Norris, J. R. (1998). *Markov chains (2nd ed.)*. Cambridge: Cambridge university press.

[24] Parshani, R., Rozenblat, C., Ietri, D., Ducruet, C., & Havlin, S. (2011). Inter-similarity between coupled networks. *EPL (Europhysics Letters), 92*(6), 68002.

[25] Pastor-Satorras, R., & Vespignani, A. (2001). Epidemic spreading in scale-free networks. *Physical Review Letters, 86*(14), 3200.

[26] Podobnik, B., Lipic, T., Horvatic, D., Majdandzic, A., Bishop, S. R., & Stanley, H. E. (2015). Predicting the lifetime of dynamic networks experiencing persistent random attacks. *Scientific Reports, 5*.

[27] Podobnik, B., Majdandzic, A., Curme, C., Qiao, Z., Zhou, W. X., Stanley, H. E., & Li, B. (2014). Network risk and forecasting power in phase-flipping dynamical networks. *Physical Review E, 89*(4), 042807.

[28] Prettejohn, B. J., Berryman, M. J., & McDonnell, M. D. (2011). Methods for generating complex networks with selected structural properties for simulations: a review and tutorial for neuroscientists. *Frontiers in Computational Neuroscience, 5*.

[29] Shang, Y. (2015). Impact of self-healing capability on network robustness. *Physical Review E, 91*(4), 042804.

[30] Shao, J., Buldyrev, S. V., Havlin, S., & Stanley, H. E. (2011). Cascade of failures in coupled network systems with multiple support-dependence relations. *Physical Review E, 83*(3), 036116.

[31] Stippinger, M., & Kertész, J. (2014). Enhancing resilience of interdependent networks by healing. *Physica A: Statistical Mechanics and its Applications, 416*, 481-487.

[32] Valdez, L. D., Di Muro, M. A., & Braunstein, L. A. (2016). Failure-recovery model with competition between failures in complex networks: a dynamical approach. *Journal of Statistical Mechanics: Theory and Experiment, 2016*(9), 093402.

[33] Valdez, L. D., Macri, P. A., Stanley, H. E., & Braunstein, L. A. (2013). Triple point in correlated interdependent networks. *Physical Review E, 88*(5), 050803.

[34] Wang, J., Jiang, C., & Qian, J. (2014). Robustness of interdependent networks with different link patterns against cascading failures. *Physica A: Statistical Mechanics and its Applications, 393*, 535-541.

[35] Watts, D. J. (2002). A simple model of global cascades on random networks. *Proceedings of the National Academy of Sciences, 99*(9), 5766-5771.

[36] Wen, X., Yang, C., Yang, Y. P., & Chen, Y. G. (2017). Phase Transition in Recovery Process of Complex Networks. *Chinese Physics Letters, 34*(5), 058901.

[37] Wilkinson, D. J. (2011). *Stochastic modelling for systems biology (2nd ed.)*. London: CRC press.

[38] Zhou, D., Stanley, H. E., D'Agostino, G., & Scala, A. (2012). Assortativity decreases the robustness of interdependent networks. *Physical Review E, 86*(6), 066103.

Appendix A

Appendix

A.1 Derivation p^*

With p^* we define the more convenient parameter for the internal failures, which reflects the fraction of internally failed nodes when there is no external failure.This parameter is different from the parameter p, which determines the rate at which node fail internally.

We assume there is no external failure, so $r = 0$ and $E = 0$, so the system in (2.13) reduces to

$$\frac{dA}{dt} = \gamma_I I - pA, \tag{A.1a}$$

$$\frac{dI}{dt} = pA - \gamma_I I. \tag{A.1b}$$

As there are no externally failed nodes we have $A + I = 1$, so equation (A.1b) can be written as follows.

$$\frac{dI}{dt} = p(1 - I) - \gamma_I I \tag{A.2}$$

This differential equation has the following steady state solution.

$$\tilde{I} = \frac{p}{p + \gamma_I} \tag{A.3}$$

For small p this can be approximated as follows.

$$\tilde{I} \approx \frac{p}{\gamma_I} \approx 1 - \exp(-\frac{p}{\gamma_I}) =: p^* \tag{A.4}$$

Note that p^* is increasing in p on its domain $[0, 1]$.

A.2 Gillespie algorithm

In the following we will discuss how the next transition and the time until the next transition is generated in step 4 and 6 of the Gillespie algorithm described in section 4.1. This discussion is based on [10]. We define

$$\begin{aligned} P(\tau, \mu)\partial\tau := \text{ probability at time } t \text{ that next transition will occur in time} \\ \text{interval}[t + \tau, t + \tau + \partial\tau] \text{ and will be the transition denoted by } \mu. \end{aligned} \tag{A.5}$$

This function is a joint probability density function on the space of continuous variable $\tau \in [0, \infty)$ and discrete variable $\mu \in \{1, \ldots, M\}$.

Define h_μ as the states that are involved in transition μ and denote the constant rate of transition μ by c_μ. For example, consider active node i with neighbors j_1, j_2 and j_3. The possible transition of active node i towards externally failed depends on the neighborhood of i. We obtain $h_\mu = (X(j_1), X(j_2), X(j_3))$ and $c_{\tilde{\mu}} = r$. We obtain the following.

$$P(\text{the next transition is } \mu \text{ during the interval of length } \partial\tau) = f(h_\mu)c_\mu\partial\tau \tag{A.6}$$

In equation (A.6) $f(h_\mu)$ is given by

$$f(h_{\tilde{\mu}}) = \begin{cases} 1 & \text{if the number of active nodes in } h_\mu \leq m, \\ 0 & \text{if the number of active nodes in } h_\mu > m.. \end{cases} \tag{A.7}$$

Next, we define

$$P_0(\tau) := \text{the probability no transition occurs in time interval } [t, t+\tau].$$

Using this expression we are able to write the probability that transition μ occurs during time interval $[t+\tau, t+\tau+\partial\tau]$ as

$$P(\tau, \mu)\partial\tau = P_0(\tau) f(h_\mu) c_\mu \partial\tau. \tag{A.8}$$

We continue with calculating $P_0(\tau)$, to do so we divide the interval of length τ in K subintervals of length ϵ, i.e. $\epsilon = \frac{\tau}{K}$. The probability that no transition occurs in interval $[t, t+\epsilon]$ is given as follows.

$$\prod_{\mu=1}^{M} \big(1 - f(h_\mu)c_\mu\epsilon + o(\epsilon)\big) = 1 - \sum_{\mu=1}^{M} f(h_\mu)c_\mu\epsilon + o(\epsilon) \tag{A.9}$$

Note that the probability that no transition occurs during $[t+\epsilon, t+2\epsilon]$, $[t+2\epsilon, t+3\epsilon]$ etc. is equal to this expression. From this follows

$$P_0(\tau) = \left(1 - \sum_{\mu=1}^{M} f(h_\mu)c_\mu\epsilon + o(\epsilon)\right)^K,$$

which can be written by substituting $\epsilon = \frac{\tau}{K}$ as,

$$P_0(\tau) = \left(1 - \frac{\sum_{\mu=1}^{M} f(h_\mu)c_\mu\tau}{K} + o(K^{-1})\right)^K.$$

If we now take the intervals infinitesimally small, i.e. $K \to \infty$ we obtain

$$P_0(\tau) = \lim_{K\to\infty} \left(1 - \frac{\sum_{\mu=1}^{M} f(h_\mu)c_\mu\tau}{K} + o(K^{-1})\right)^K \tag{A.10}$$

$$P_0(\tau) = \exp\left(-\sum_{\mu=1}^{M} f(h_\mu)c_\mu\tau\right). \tag{A.11}$$

In the last line we used the standard limit for the exponential formula, substituting this expression in equation (A.8) yields

$$\begin{aligned} P(\tau, \mu) &= \exp\left(-\sum_{v=1}^{M} f(h_v)c_v\tau\right) f(h_\mu)c_\mu\partial\tau, \\ P(\tau, \mu) &= a_\mu \exp(-a\tau), \end{aligned} \tag{A.12}$$

where we used the abbreviated notations

$$a_\mu = f(h_\mu)c_\mu \qquad \text{and} \qquad a = \sum_{\mu=1}^{M} a_\mu. \tag{A.13}$$

Equation (A.12) gives for input $\tau \in [0, \infty)$ and $\mu \in \{1, \ldots, M\}$ the probability that the transition during the next time interval of length τ is μ. We aim to generate two uniform random numbers τ, μ according to the probability density function $P(\tau, \mu)$. First we condition the function on τ, we obtain

$$P(\tau, \mu) = P_1(\tau)P_2(\mu|\tau). \tag{A.14}$$

In this equation $P_1(\tau)$ is the probability that the next transition occurs in the interval $[t+\tau, t+\tau+\partial\tau]$, independent of the transition. Also $P_2(\tau|\mu)$ is the probability that μ is the next transition given that it occurs at time $t+\tau$. We have

$$P_1(\tau) = \sum_{\mu=1}^{M} P(\tau, \mu), \tag{A.15}$$

substituting this equation in equation (A.14) and solving to $P_2(\mu|\tau)$ yields

$$P_2(\mu|\tau) = \frac{P(\tau, \mu)}{\sum_{\mu=1}^{M} P(\tau, \mu)}. \tag{A.16}$$

Substituting the expression for $P(\tau, \mu)$ of equation (A.12) in equation (A.15) gives

$$P_1(\tau) = \sum_{\mu=1}^{M} a_\mu \exp(-a\tau) = a\exp(-a\tau), \tag{A.17}$$

$$P_2(\mu|\tau) = \frac{a_\mu \exp(-a\tau)}{a\exp(-a\tau)} = \frac{a_\mu}{a}. \tag{A.18}$$

We check that P_1 and P_2 are normalized by integrating $P_1(\tau)$ over its continuous domain for τ ($[0, \infty)$) and summing $P_2(\mu|\tau)$ over its discrete domain for μ ($\{1, \ldots, M\}$):

$$\int_0^\infty P_1(\tau)\partial\tau = \int_0^\infty a\exp(-a\tau)\partial\tau = 1,$$

$$\sum_{\mu=1}^{M} P_2(\mu|\tau) = \sum_{\mu=1}^{M} \frac{a_\mu}{a} = 1.$$

We recognize in equation (A.17) the probability distribution function P with mean a. The cummulative distribution function of P_1 is then given by

$$F(\tau, a) = 1 - \exp(-a\tau) \qquad \text{for } \tau \geq 0. \tag{A.19}$$

Drawing a random number τ from the exponential distribution with mean a goes as follows. First we draw a number $1 - z_1$ from the uniform distribution on the unit interval, notice that this is the same as drawing a number z_1. For τ we take the value that satisfies $F(\tau, a) = 1 - z_1$. From this follows

$$\tau = -\frac{1}{a}\ln(\frac{1}{z_1}) \tag{A.20}$$

Next in equation (A.18) we recognize the uniform distribution on interval $[0, a]$. So μ can be drawn by generating a random number z_2 on the unit interval and take μ the transition that satisfies

$$\frac{\sum_{v=1}^{\mu-1} a_v}{a} \leq z_2 \leq \frac{\sum_{v=1}^{\mu} a_v}{a}. \tag{A.21}$$

Remark that it is important to have a reliable random number generator, for a discussion see section 4.3 of [37]. As this topic is beyond the scope of this thesis we will not be concerned with the precise method to generate random numbers but take the random numbers as a starting point of our algorithm.

A.3 Interconnected networks

A.3.1 Derivation mean field equations

Before we derive the mean field equations from the system of ODEs, as in equations (3.3) to (3.6), we state the following lemma.

Lemma 3. *For $a, i, e, d \in \mathbb{N}$ such that $a + i + e + d \in [0, k_{max}]$*

$$\sum_{a=0}^{k_{max}} \sum_{i=0}^{k_{max}} \sum_{e=0}^{k_{max}} \sum_{d=0}^{k_{max}} \big((a+1)X(a+1, i-1, e, d) - aX(a, i, e, d)\big) = 0. \tag{A.22}$$

We omit the proof of lemma 3 as it is similar to the proof of lemma 1. Next we derive the mean field equations by summing equations (3.3) to (3.6) over a, i, e, d. Applying lemma 3 makes sure a lot of terms cancel out, this is what we have also seen in the case of single networks. We obtain the following set of mean field equations.

$$\frac{dA^A}{dt} = \gamma_I I^A + \gamma_E E^A - p_A A^A - r_A \sum_{a=0}^{m} \sum_{i=0}^{k_{max}} \sum_{e=0}^{k_{max}} \sum_{e=0}^{k_{max}} A^A(a,i,e,d) + \gamma_D D^A - r_D(1-A^B) \tag{A.23a}$$

$$\frac{dI^A}{dt} = p_A A^A - \gamma_I I^A \tag{A.23b}$$

$$\frac{dE^A}{dt} = r_A \sum_{a=0}^{m} \sum_{i=0}^{k_{max}} \sum_{e=0}^{k_{max}} \sum_{e=0}^{k_{max}} A^A(a,i,e,d) - \gamma_E E^A \tag{A.23c}$$

$$\frac{dD^A}{dt} = r_D(1-A^B) - \gamma_D D^A \tag{A.23d}$$

We continue with a lemma that approximates the fraction of active nodes in network A.

Lemma 4. *For a network with arbitrary degree distribution $f(k)$ we obtain the following mean field approximation.*

$$\sum_{a=0}^{m} \sum_{i=0}^{k_{max}} \sum_{e=0}^{k_{max}} \sum_{d=0}^{k_{max}} A^A(a,i,e,d) = A^A \sum_k f(k) \sum_{j=0}^{m} \binom{k}{j} (1-A^A)^{k-j} (A^A)^j \tag{A.24}$$

Note that this lemma is lemma 2 for the new state space, therefore we omit the proof. Substituting the approximation of lemma 4 in equations (A.23a) to (A.23d) gives the system of mean field equations.

$$\begin{aligned}\frac{dA^A}{dt} = \gamma_I I^A + \gamma_E E^A - p_A A^A - r_A A^A \sum_k f(k) \sum_{j=0}^{m} \binom{k}{j} (1-A^A)^{k-j} (A^A)^j \\ + \gamma_D D^A - r_D(1-A^B)\end{aligned} \tag{A.25a}$$

$$\frac{dI^A}{dt} = p_A A^A - \gamma_I I^A \tag{A.25b}$$

$$\frac{dE^A}{dt} = r_A A^A \sum_k f(k) \sum_{j=0}^{m} \binom{k}{j} (1-(A^A))^{k-j} (A^A)^j - \gamma_E E^A \tag{A.25c}$$

$$\frac{dD^A}{dt} = r_D^A(1-A^B) - \gamma_D D^A \tag{A.25d}$$

We only listed the mean field equations for network A, by replacing the superscripts of the state variables and the subscripts of the constants A (B) by B (A) we obtain the full system of mean field equations.

In equations (A.25a) to (A.25d) we derived the system of mean field equations, now we will find the fixed points of this system and investigate their stability. Since $E = 1 - A - I - D$ we only consider equations (A.25a), (A.25b) and (A.25d) and use the substitution $E = 1 - I - A - D$, this leads to three differential equations in three unknown for network A as in equation (A.26) .

$$\begin{aligned}\frac{dA^A}{dt} = \gamma_I I^A + \gamma_E(1 - A^A - I^A - D^A) - p_A A^A - r_A A^A \sum_k f(k) \sum_{j=0}^{m} \binom{k}{j} (1-A^A)^{k-j} (A^A)^j \\ + \gamma_D D^A - r_D(1-A^B)\end{aligned} \tag{A.26a}$$

$$\frac{dI^A}{dt} = p_A A^A - \gamma_I I^A \tag{A.26b}$$

$$\frac{dD^A}{dt} = r_D(1-A^B) - \gamma_D D^A \tag{A.26c}$$

From this system the steady state solution for I and D are given by

$$\tilde{I^A} = \frac{p}{\gamma_I} A^A \qquad \text{and} \qquad \tilde{D^A} = \frac{r_D}{\gamma_D}(1-A^B). \tag{A.27}$$

Next, we substitute this steady state solutions in equation (A.26a). We obtain the following.

$$\frac{dA^A}{dt} = \gamma_I \left(\frac{p_A}{\gamma_I} A^A\right) + \gamma_E \left(1 - A^A - \frac{p_A}{\gamma_I} A^A - \left(\frac{r_D}{\gamma_D}(1 - A^B)\right)\right) - pA^A$$
$$- r_A A^A \sum_k f(k) \sum_{j=0}^{m} \binom{k}{j} (1 - A^A)^{k-j} (A^A)^j + \gamma_D \left(\frac{r_D}{\gamma_D}\left(1 - A^B\right)\right) - r_D(1 - A^B) \tag{A.28}$$

From this follows the equation that is satisfied in the steady state in equation (A.29) or equivalently equation (A.30).

$$0 = \gamma_E \left(1 - A^A - \frac{p_A}{\gamma_I} A^A - \left(\frac{r_D}{\gamma_D}\left(1 - A^B\right)\right)\right) - r_A A^A \sum_k f(k) \sum_{j=0}^{m} \binom{k}{j} (1 - A^A)^{k-j} (A^A)^j \tag{A.29}$$

$$A^A = 1 - \frac{p_A}{\gamma_I} A^A - \frac{r_A}{\gamma_E} A^A \sum_k f(k) \sum_{j=0}^{m} \binom{m}{j} (1 - A^A)^{k-j} (A^A)^j - \frac{r_D}{\gamma_D}(1 - A^B) \tag{A.30}$$

For the other network we obtain a similar result. So we obtain a set of two differential equations that are satisfied in the steady state as follows.

$$A^A = 1 - \frac{p_A}{\gamma_I} A^A - \frac{r_A}{\gamma_E} A^A \sum_k f(k) \sum_{j=0}^{m} \binom{m}{j} (1 - A^A)^{k-j} (A^A)^j - \frac{r_D}{\gamma_D}(1 - A^B) \tag{A.31a}$$

$$A^B = 1 - \frac{p_B}{\gamma_I} A^B - \frac{r_B}{\gamma_E} A^B \sum_k f(k) \sum_{j=0}^{m} \binom{m}{j} (1 - A^B)^{k-j} (A^B)^j - \frac{r_D}{\gamma_D}(1 - A^A) \tag{A.31b}$$

A.3.2 Linearization

In what follows we will linearize the system, as in equation (A.26), around the fixed points obtained by equation (A.31). Suppose $\left(\overline{A^A}, \overline{I^A}, \overline{D^A}, \overline{A^B}, \overline{I^B}, \overline{D^B}\right)$ is a fixed point of the system

$$(f_1, f_2, f_3, g_1, g_2, g_3) := \left(\frac{dA^A}{dt}, \frac{dI^A}{dt}, \frac{dD^A}{dt}, \frac{dA^B}{dt}, \frac{dI^B}{dt}, \frac{dD^B}{dt}\right). \tag{A.32}$$

Then the linearized system is given by

$$\begin{pmatrix} \dot{u}^A \\ \dot{v}^A \\ \dot{w}^A \\ \dot{u}^B \\ \dot{v}^B \\ \dot{w}^B \end{pmatrix} = J \begin{pmatrix} u^A \\ v^A \\ w^A \\ u^B \\ v^B \\ w^B \end{pmatrix}, \tag{A.33}$$

where $u^A = A^A - \overline{A^A}, v^A = I^A - \overline{I^A}, w^A = D^A - \overline{D^A}, u^B = A^B - \overline{A^B}, v^B = I^B - \overline{I^B}$ and $w^B = D^B - \overline{D^B}$. The Jacobian J is given by

$$J = \begin{pmatrix} -\gamma_E - p_A - r_A \mathbf{s}(A^A) & \gamma_I - \gamma_E & -\gamma_E + \gamma_D & r_D & 0 & 0 \\ p_A & -\gamma_I & 0 & 0 & 0 & 0 \\ 0 & 0 & -\gamma_D & -r_D & 0 & 0 \\ r_D & 0 & 0 & -\gamma_E - p_B - r_B \mathbf{s}(A^B) & \gamma_I - \gamma_E & -\gamma_E + \gamma_D \\ 0 & 0 & 0 & p_B & -\gamma_I & 0 \\ -r_D & 0 & 0 & 0 & 0 & -\gamma_D \end{pmatrix}, \tag{A.34}$$

with

$$\mathbf{s}(A) = \sum_k f_k \sum_j \binom{k}{j} \left((j+1)A^j(1-A)^{k-j} - (k-j)(1-A)^{k-j-1}A^{j+1}\right).$$